



Soft-sediment deformation within seismogenic slumps of the Dead Sea Basin

G.I. Alsop^{a,*}, Shmuel Marco^b

^a Department of Geology and Petroleum Geology, School of Geosciences, University of Aberdeen, Aberdeen AB24 3UE, UK

^b Department of Geophysics and Planetary Sciences, Tel Aviv University, Tel Aviv 69978, Israel

ARTICLE INFO

Article history:

Received 6 October 2010

Received in revised form

11 February 2011

Accepted 14 February 2011

Available online 19 February 2011

Keywords:

Slump

Folds

Earthquakes

Mass transport complexes

Gravity-driven deformation

Dead Sea Basin

ABSTRACT

The Late Pleistocene Lisan Formation preserved next to the Dead Sea provides exceptional 3-D exposures of folds and faults generated during soft-sediment slumping and deformation. It is possible to generate a range of four different scenarios associated with overprinting in a single slump event. The progressive evolution of slump systems may be broadly categorised into initiation, translation, cessation, relaxation and compaction phases. Thrust packages typically define piggyback sequences during slump translation, with back-steepening of imbricate faults leading to collapse of folds back up the regional palaeoslope. Detailed evaluation of slumped horizons may also permit structures to be traced across apparently separate and distinct slumped units. The recognition that slumps may be reworked by younger seismically-triggered events suggests that in some cases the seismic recurrence interval may be shorter than previously anticipated.

© 2011 Elsevier Ltd. All rights reserved.

1. Introduction

Folds and faults related to slumping are perhaps the most conspicuous of gravity-driven structures in unconsolidated or soft-sediments, and are considered to be the only structures that primarily reflect the orientation of the palaeoslope in ancient settings (see reviews in Woodcock, 1976a, b, 1979; Maltman, 1984, 1994a, b; Collinson, 1994; Strachan and Alsop, 2006; Debacker et al., 2001, 2009; Waldron and Gagnon, 2011). However, a number of text books give the impression that soft-sediment slump folds are rather disorganised and lack meaningful pattern. For instance, Davis and Reynolds (1996, p. 658) suggest that within slumps “folds do not propagate upward or downward in any systematic, predictable manner”, while Van der Pluijm and Marshak (2004, p. 24) describe slump folds as “characteristically chaotic” displaying “little symmetry” with folds in one layer of “a different size and orientation than the structures in adjacent layers”. We suggest that, with careful and systematic structural analysis, coherent and meaningful patterns do emerge which enable a greater understanding of the deformation processes and mechanisms. In addition, a greater appreciation of the structural complexities that may arise during the slumping process may not

only enable a better understanding of large-scale mass transport complexes (e.g. see review by Bull et al., 2009) and their associated palaeogeographies, but also of the nature and style of deformation associated with processes of flow in general. Clearly, this may have applications beyond sedimentary slumps in other settings in which lateral flow of material occurs such as subglacial shear zones (e.g. see review and references in Lesemann et al., 2010), snow slides (e.g. Lajoie, 1972), salt glaciers (e.g. see review and references in Aftabi et al., 2010) and mid-crustal shear zones (e.g. see review and references in Druguet et al., 2009).

Our study aims to explore a number of fundamental questions and factors pertaining to slumped sediments. These include the structural analysis of deformation sequences developed during slumping, together with the possible recognition of multiple slump events and reworking within individual slumped horizons. In addition, the direct examination of small scale structures developed during slumping may provide additional constraints on larger scale gravity-driven linked extensional-contractional systems in which elements of contraction are apparently “missing” when attempts to balance extension – contraction on seismic sections are made (e.g. see Butler and Paton, 2010 and references therein). In order to address these issues we provide a detailed case study together with new observations and data from late-Pleistocene sediments exposed on the western margin of the Dead Sea. To place these observations in context, we start by providing an overview of interpretational models relating to slumped systems.

* Corresponding author.

E-mail address: Ian.Alsop@abdn.ac.uk (G.I. Alsop).

2. Models of folding and faulting in slumped sediments

Gravity-driven slumps have been hypothetically modelled by a number of authors in terms of deformation cells associated with extension in the upper parts balanced by contraction in the lower parts of the slump (e.g. Hansen, 1971; Lewis, 1971; Farrell, 1984; Farrell and Eaton, 1987; Elliot and Williams, 1988; Martinsen, 1989, 1994; Martinsen and Bakken, 1990; Smith, 2000; Strachan, 2002) (Fig. 1a). Within these interpretational models, slump sheet movement or translation occurs along an underlying detachment, with extension at the head of the slump propagating upslope, whilst contraction at the toe of the slump propagates downslope. The lateral margins of the slump are interpreted as zones of differential movement associated with strike-slip deformation that are broadly parallel to the overall downslope direction of movement

(Fig. 1a) (Farrell, 1984; Debacker et al., 2009). Extension at the head of the slump is marked by normal faulting, with younger extensional faults forming in the footwall of existing faults (thereby propagating upslope), while contractional folds and thrusts at the toe also form a piggyback system (Fig. 1a). Piggyback thrusting is marked by new material being incorporated and accreted into the leading edge of the thrust system, resulting in a progressive back-rotation and steepening of existing thrusts (Fig. 1a).

If slump translation first starts to slow down and cease at the toe of the slump, then a wave of contractional strain is interpreted to propagate upslope back through the slump sheet (Farrell, 1984) (Fig. 1b). This may generate new thrusts that sequentially develop upslope with the propagating strain wave in an overstep sequence (Fig. 1b), together with possible reactivation and overprinting of existing structures. Overstep thrusting is marked by new thrusts

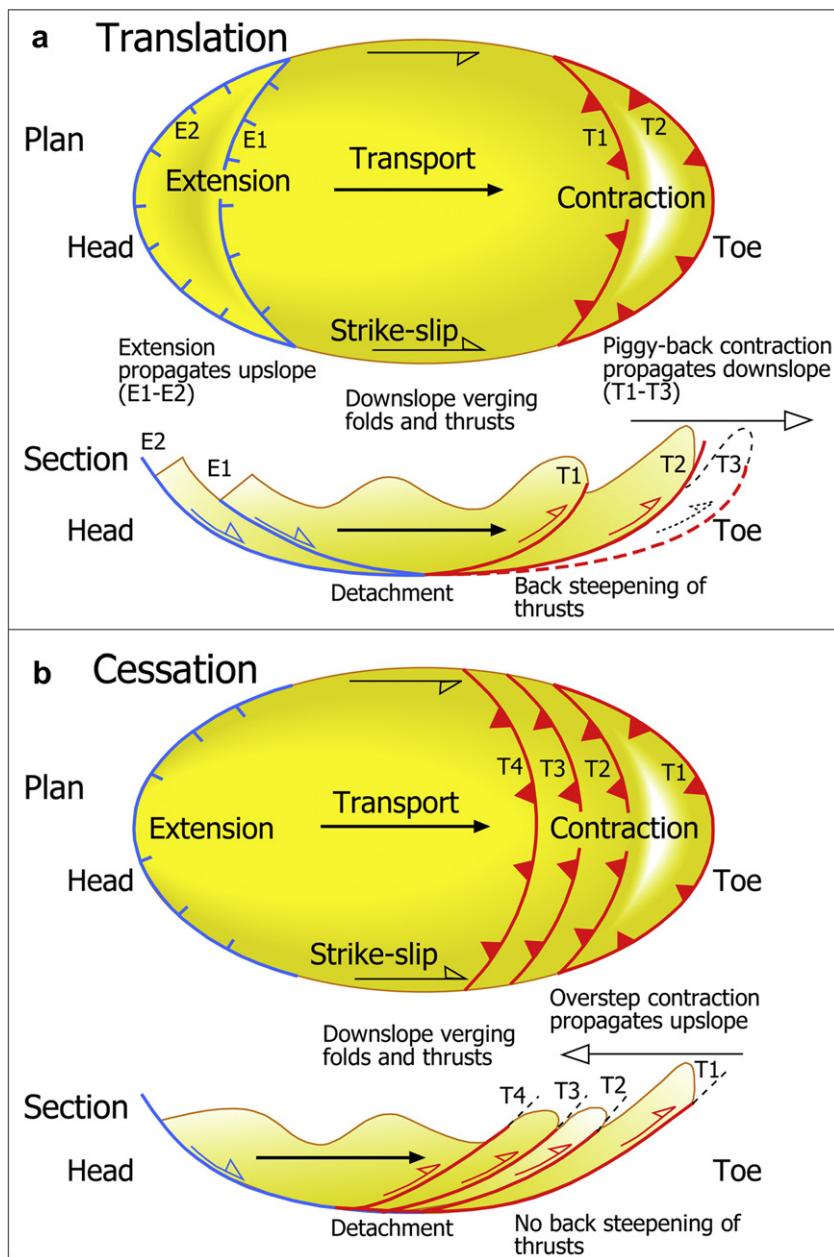


Fig. 1. Schematic plan view (above) and cross section (below) of contractional, extensional and strike-slip structures generated within a slump during its translation a), and its subsequent cessation b). Within these interpretational models, the direction of transport associated with flow from left to right is shown by the black arrow, with sequential contractional thrusts (T1, T2 etc) shown in red at the toe of the slump and extensional faults (E1, E2) shown in blue at the head.

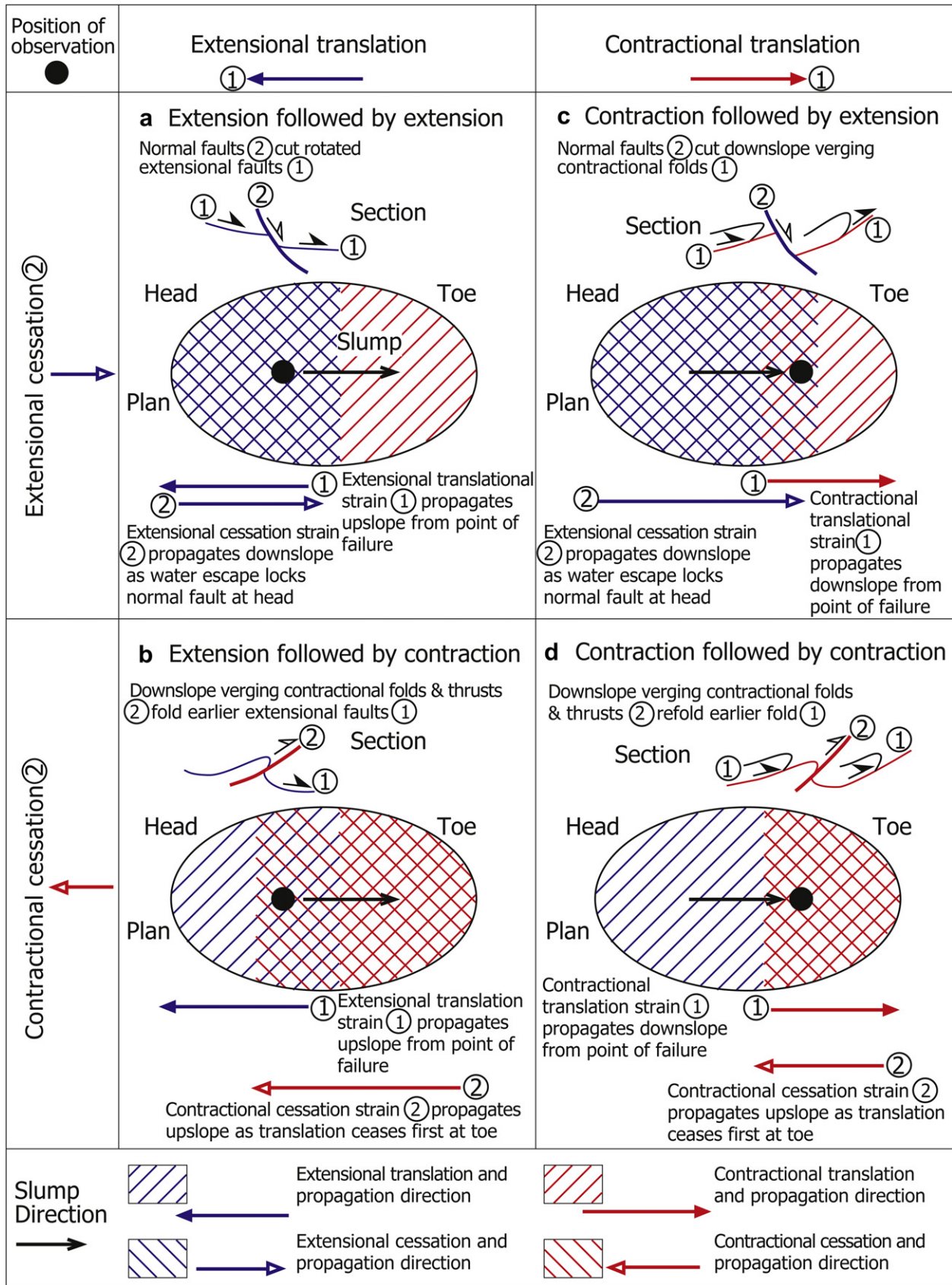


Fig. 2. Schematic plan view maps and associated sections of extensional (blue) and contractional (red) structures generated during translation (1) and subsequent cessation (2) of slump sheets. In each model, the position of observations is marked by the black circle while the slump translates from left (head) to right (toe) (shown by black arrow). While the figure illustrates the four end-member scenarios (a–d), it should be noted that the lateral margins of the slump sheet may also display complex differential movement associated with strike-slip deformation.

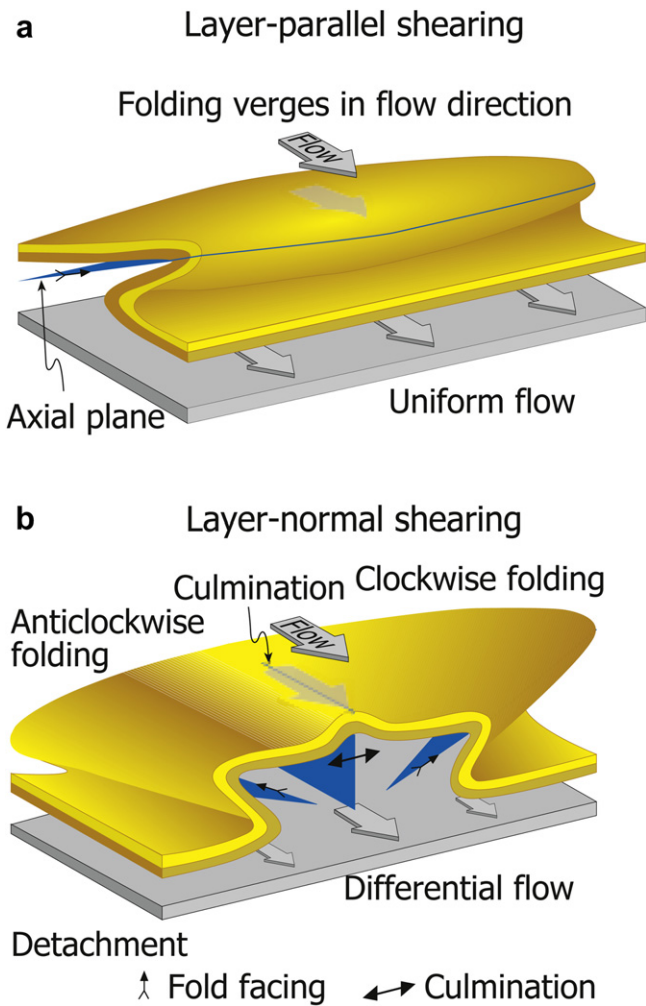


Fig. 3. a) During layer-parallel shearing (LPS), uniform flow along an underlying detachment (shown by flow arrows) generates folds that are broadly flow-normal and verging and facing upwards in the flow direction. Axial planes (shown in blue) typically dip and fan about the normal to the flow direction i.e. parallel to the strike of the palaeoslope. b) During layer-normal shearing (LNS), differential flow along an underlying detachment (shown by variable sized flow arrows) generates folds in the overlying sequence that may be anticlockwise or clockwise of flow where associated with a dextral or sinistral differential component respectively. Axial planes (shown in blue) and associated facing directions typically fan about the flow direction, and may also create culminations sub-parallel to flow.

forming in the hangingwall of older thrusts, and although the thrust system still verges downslope, there is no pronounced back steepening of older structures that may themselves be cut by the newer overlying thrusts (Fig. 1b). If slump translation first starts to slow down and cease at the head of the slump, possibly due to water

escape along normal faults (Farrell, 1984), then an extensional strain wave will propagate down through the slump during its cessation.

Depending on the exact location of observations within a slump sheet, it is therefore theoretically possible to generate four end-member overprinting scenarios associated with translation and cessation structures (Fig. 2). Structures associated with slump translation may be either extensional (at the head, Fig. 2a, b) or contractional (at the toe Fig. 2c, d) and these may be overprinted by structures associated with extensional cessation (if the slump system locks first at the head), or contractional cessation (if the system locks first at the toe) (Fig. 2). Farrell (1984) notes that overprinting of extensional faults by contractional folds and thrusts is the less common of these scenarios, although this may also reflect the inherent difficulty in distinguishing early extensional faults that are frequently sub-parallel to bedding. Strachan and Alsop (2006) record early recumbent folds being refolded by later upright folds, suggesting a late-stage contractional overprint of earlier folds related to translation. Although extensional and contractional deformation are schematically shown as being of approximately equivalent areas on Fig. 2, the area of extensionally strained sediment at the head (rear) of a slump sheet is typically modelled as being much greater than the area of contractional strain concentrated towards the toe (Farrell, 1984). Clearly a range of distinct overprinting relationships is theoretically possible, although multiple phases of like deformation (e.g. extensional structures related to both translation and cessation) are more difficult to distinguish. In addition, differential shear at the lateral margins of slump sheets will theoretically create further complexity in these areas. However, such differential shear zones are not observed in the present case study (discussed in Section 7.5) and we therefore focus our attention on folding and faulting associated with contractional and extensional deformation.

2.1. General patterns of flow perturbation folding within slump sheets

Folds and faults developed within slump sheets may be analysed in terms of general flow perturbation models frequently applied to deformation in metamorphic rocks (e.g. Coward and Potts, 1983; Ridley, 1986; Holdsworth, 1990; Alsop and Holdsworth, 2004a, b). Folds generated during translation of a slump sheet typically define broadly arcuate traces about the flow (downslope) direction reflecting variations in movement on the underlying detachment (e.g. Farrell, 1984; Alsop and Holdsworth, 2002, 2007; Strachan and Alsop, 2006). Velocity (and hence shear strain) gradients in the downslope (flow) direction will generate layer-parallel shear (LPS) in the slump with folds forming at high angles to flow (Fig. 3a), while velocity gradients along the strike of the palaeoslope will create differential layer-normal shear (LNS) with folds initiating oblique or even sub-parallel to flow (Fig. 3b) (Alsop and Holdsworth, 2002, 2007; Strachan and Alsop, 2006; Debacker et al., 2009) (Table 1).

Table 1
Summary of Layer Parallel Shear (LPS) and Layer Normal Shear (LNS) criteria.

| | Layer Parallel Shear (LPS) | Layer Normal Shear (LNS) |
|-------------------------|--|--|
| Fold hinge orientation | Transport normal (parallel strike of slope) | Transport sub-parallel (parallel dip of slope) |
| Fold hinge vergence | Unimodal vergence pattern (parallel dip of slope) | Bimodal vergence pattern (parallel strike of slope) |
| Fold axial plane strike | Varies about transport normal (intersections parallel strike of slope) | Varies about transport direction (intersections parallel dip of slope) |
| Fold axial plane dips | Unimodal axial planar dip distribution with few dipping downslope. Dips fan about transport normal with intersections parallel strike of slope. | Bimodal axial planar dip distribution with equal numbers dipping either way. Dips fan about transport direction with intersections parallel dip of slope. |
| Fold Facing direction | Unimodal (upwards) facing pattern about transport direction. (facing direction parallel dip of slope) | Bimodal (upwards) facing pattern about transport normal (facing directions parallel strike of slope) |

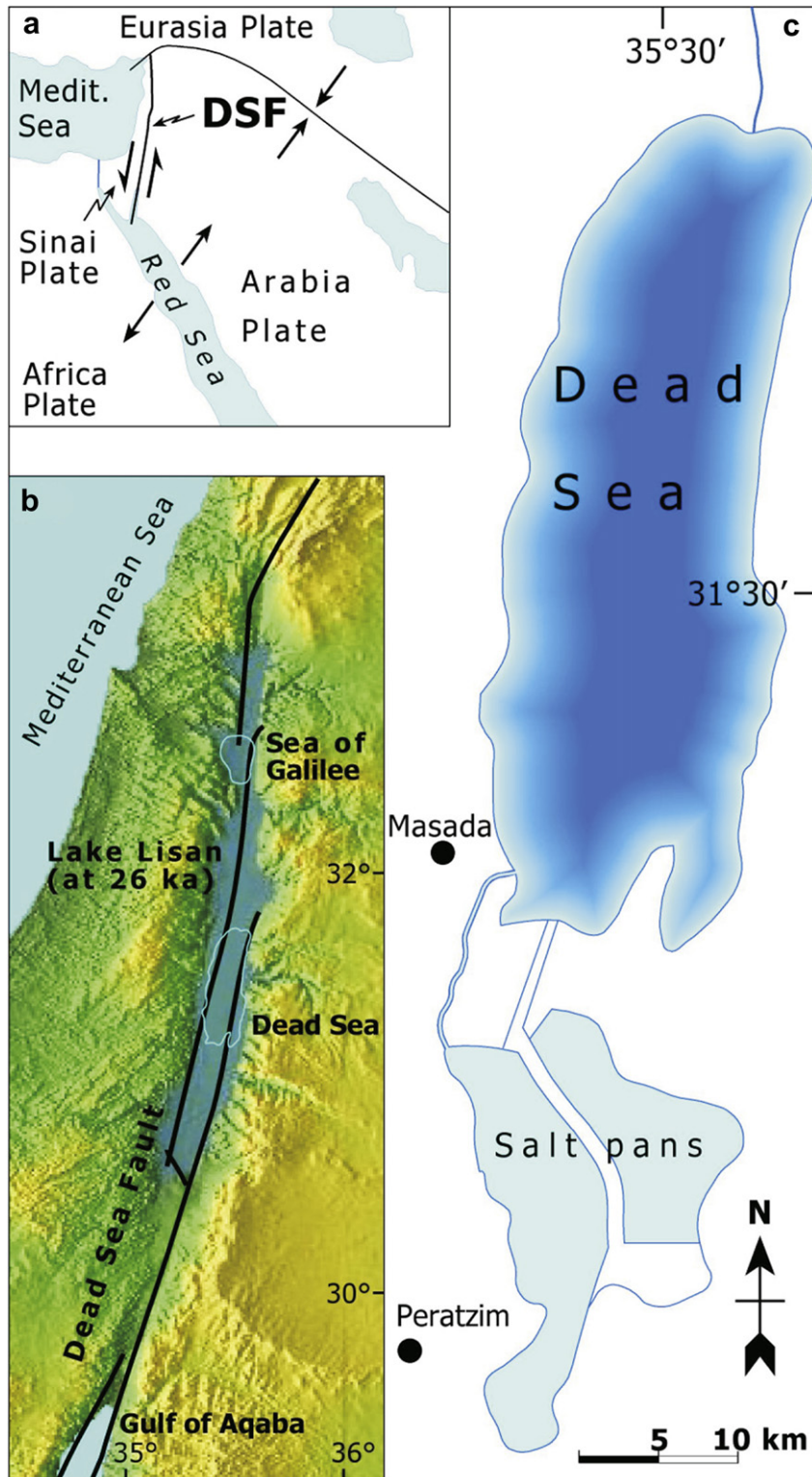


Fig. 4. a) Tectonic plates in the Middle East. General tectonic map showing the location of the present Dead Sea Fault (DSF). The Dead Sea Fault transfers the opening motion in the Red Sea to the Taurus–Zagros collision zone. b) Generalised map showing the maximum extent of Lake Lisan along the Dead Sea Fault at 26 Ka. c) Map of the current Dead Sea showing the positions of Peratzim and Masada referred to in the text.

It should also be noted that shear-strain gradients in the downslope flow direction may, in addition to layer-parallel simple shear, also lead to layer-parallel pure-shear shortening (or extension). Folds initiating at high angles to palaeoslope during LPS will display unimodal (downslope) vergence patterns and axial planes that dip

in the upslope direction (Woodcock, 1979), but which progressively rotate during continued downslope slumping to create statistical fans about the transport normal (Fig. 3a, Table 1). Conversely, folds initiating oblique or sub-parallel to palaeoslope during LNS will be marked by bimodal vergence patterns and axial planes that



Fig. 5. Field photographs of sub-vertical sedimentary injections cross cutting horizontal beds and NE-thrusted slumped horizons at Peratzim. a) Note the stepping and

statistically fan directly about the transport direction (Fig. 3b, Table 1). It should be noted that both fold hinges and axial planes may undergo rotation during progressive shearing to create sheath folds which will complicate vergence patterns (Alsop and Holdsworth, 2006; Alsop et al., 2007; Alsop and Carreras, 2007).

2.2. General patterns of fold facing within slump sheets

In addition to measurements of fold orientation and vergence, the concept of fold facing may also be applied. Facing is defined as the direction, normal to the fold hinge and along the axial plane, in which younger beds are encountered (see Holdsworth, 1988). Facing is therefore a directional measurement with an upward or downward component. Woodcock (1976a) recognised that slump folds will typically be upwards facing towards the downslope slump direction. It is important to note therefore that downward facing folds are, in general, atypical and may involve a degree of reworking where originally upward facing folds are rotated into downward facing orientations related to either classic refolding or thrust ramp geometries. Within slump systems dominated by layer-parallel shear (LPS), the fold hinges and associated axial planes form parallel to the palaeoslope with the facing direction therefore typically upwards and parallel to the downslope slump direction (Fig. 3a, Table 1). Conversely, in slump systems dominated by layer-normal shear (LNS), the fold hinges and associated axial planes form normal to the palaeoslope with the facing direction therefore typically upwards and normal to the downslope direction (Fig. 3b, Table 1).

Within most slump sheets, the assumption is that deformation largely relates to layer-parallel shearing (LPS) while differential layer-normal shearing (LNS) is largely restricted to the marginal strike-slip zones (see Alsop and Holdsworth, 2007; Debacker et al., 2009) (Fig. 3a, b, Table 1). Variable combinations of LPS and LNS will thus create a range of arcuate fold and facing patterns within the slump sheet (see review in Alsop and Holdsworth, 2007). However, the relative components of LPS and LNS will also depend on the overall shape and extent of the slump sheet (i.e. how far it extends along-strike compared to downslope) together with the nature of LPS and LNS partitioning, which may be dependent on the inter-layered properties and character of the sediment. We now present new data and observations from the Dead Sea with which to further constrain models of slump evolution.

3. Geological setting of the Dead Sea case study

3.1. Justification of the case study area

The Dead Sea Basin is an ideal place to study and analyse details of slumping processes as this is a relatively recent and simple system that fulfils a number of requirements and criteria that aid in the general clarification of soft-sediment slumping. These include:

3.1.1. An obvious mechanism to trigger slumping

The Dead Sea sits astride the Dead Sea transform that provides a long and remarkable palaeoseismic record (Marco et al., 1996; Ken-Tor et al., 2001; Migowski et al., 2004) (Fig. 4a, b).

en-echelon fracture-filling nature of injections, which are sourced from the directly underlying mud-rich slumped unit. b) Sub-vertical injection cross cutting NE-directed folds and thrusts and overlying more chaotic brecciated horizon. The injection steps to the right (NE) when cutting the mud-rich marker bed. This deformed horizon is overlain by undeformed horizontal beds that cap the slump and are also cut by the sedimentary injection. c) Sub-vertical injection that cuts a slumped unit and overlying more chaotic beds. The slumped horizon is overlain by horizontal beds that are also cut by the injection.

Earthquakes associated with this plate boundary provide a clear and obvious seismic trigger to generate sedimentary slumps.

3.1.2. An identifiable palaeogeography to drive slumping

The present exceptional Dead Sea bathymetry reaches ~ -750 m below sea level and not only controls the current depocentre, but is also considered to dominate the palaeogeography of the older late Pleistocene deposits that form the focus of the present study.

3.1.3. A refined stratigraphic template to record slumping

Annual varve-like laminations in the Lisan marls are developed on a mm scale and comprise aragonite-rich and clastic detritus-rich pairings representing summer and winter seasons respectively (Begin et al., 1974). These couplets provide an extremely fine and effective layer-cake stratigraphic template upon which to record the effects of deformation.

3.1.4. A lack of late tectonics to preserve slumping

No post-slumping tilting or deformation of late Pleistocene beds has occurred because post- and intra-slump beds remain sub-horizontal ($<1^\circ$ dips). Slumped units therefore retain pristine structural relationships uncomplicated by later tectonics.

3.1.5. Preserved upper and lower contacts to restore slumping

Exposed upper and lower contacts to slumped horizons are routinely observed (e.g. Fig. 5a). In the present case study these

display depositional dip of $<1^\circ$, but in other examples these bounding contacts provide a “stratigraphic reference frame” (Bradley and Hanson, 1998) that would critically permit the identification of a palaeohorizontal and hence constrain rotation and restoration of structural elements to original attitudes.

3.1.6. A lack of bioturbation to preserve slumping

The exceptional salinity and anoxic bottom of Lake Lisan (and the Dead Sea) provides lifeless lakebed conditions that ensure a lack of bioturbation within sediments. This allows the Lisan Formation sediments to preserve exceptional sedimentary features related to slumping.

3.1.7. Unambiguous stratigraphic relationships to verify slumping

Undeformed sequences of horizontal sediments cap each slumped unit thereby providing clear evidence that structures are soft-sediment and slump generated rather than related to any later tectonic deformation of lithified sequences (e.g. Fig. 5a, b, c).

3.1.8. Unambiguous structural relationships to verify slumping

Sub-horizontal slump sequences are cross cut by sub-vertical sedimentary injections sourced from underlying horizons (Fig. 5a). This provides clear evidence that the folds and thrusts are related to slumping and developed prior to complete lithification of the underlying sequence. Resetting of quartz Optically Stimulated Luminescence (OSL) suggests sedimentary injections occurred

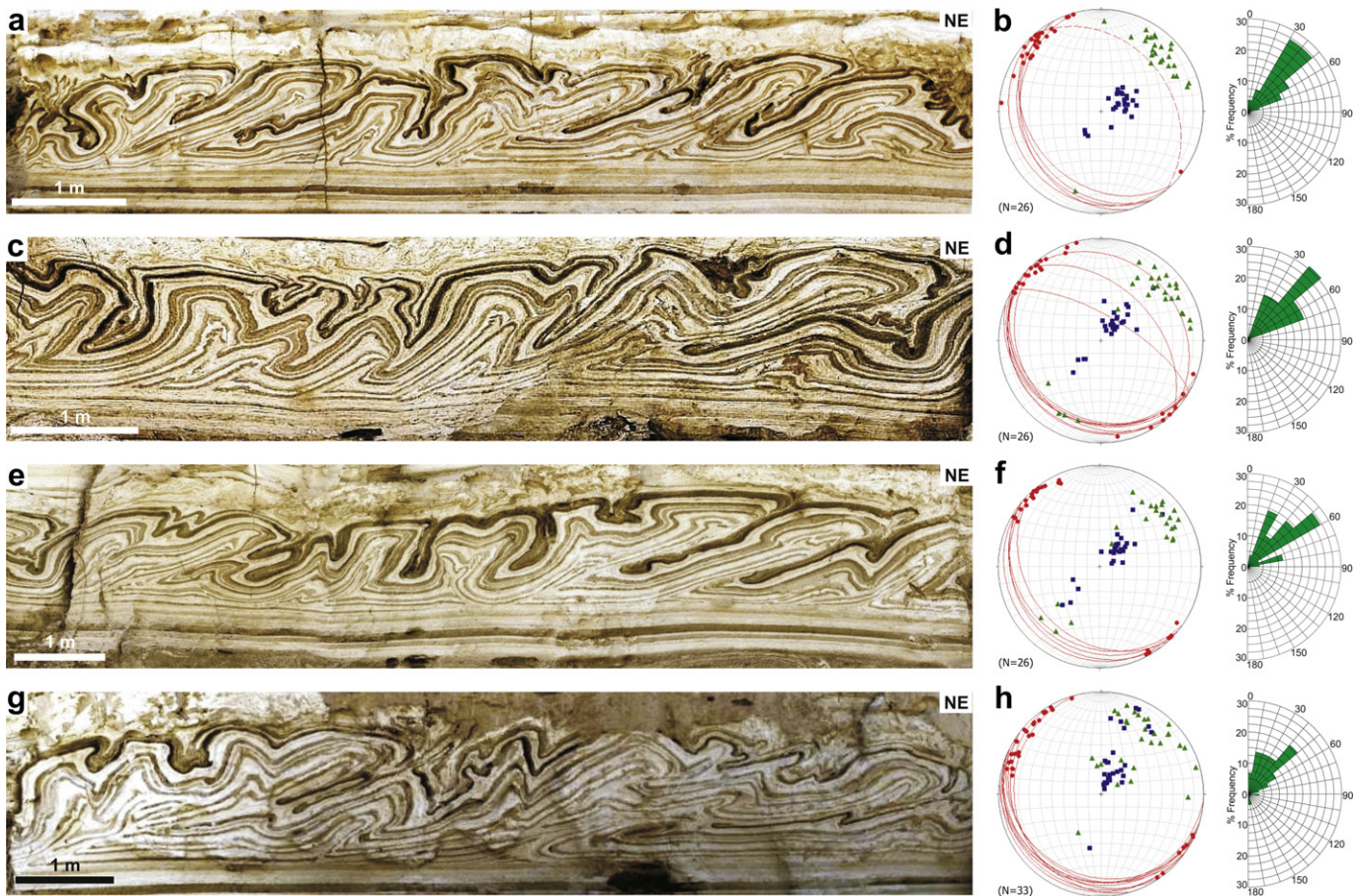


Fig. 6. Photographs and associated structural data pairings (a–b, c–d, e–f, g–h) from a single continuous slumped unit at Peratzim. Equal area stereoplots are of fold hinges (red circles), thrusts (red great circles) and axial surfaces (blue squares). As lines of upward facing project onto the upper hemisphere of a stereonet, they are plotted as chordal points (green triangles) on the standard lower hemisphere stereonet (i.e. intersections on the upper hemisphere are simply projected vertically down from the upper to lower hemispheres). Facing trends are also shown on the associated rose diagrams, and are typically parallel to the inferred NE-directed slump transport. Refer to Fig. 10 for the complete section.

between 15 and 7 Ka (Porat et al., 2007), with propagation velocities of $\sim 4\text{--}65$ m/s over intervals of 0.8–2 s (Levi et al., 2011).

3.1.9. Well exposed and accessible sections to observe slumping

The slumped units are exposed on the numerous walls of wadi systems generated by sporadic flash floods. In addition, annual drops of ~ 1 m/year in the level of the Dead Sea (possibly linked to salt pan activity, water extraction and increasing aridity) continue to drive deep incision resulting in well-exposed canyons through the Lisan marls.

3.2. Tectonic setting and sedimentology of the Lisan formation

The Late Pleistocene (70–15 Ka) Lisan Formation comprises a sequence of laminated muds and carbonates (Haase-Schramm et al., 2004). It was deposited in a lake, which occupied an elongate tectonic depression formed where the Dead Sea Fault (DSF) is made of two parallel strands (Garfunkel, 1981) (Fig. 4a, b). Recent seismic activity as well as abundant historical accounts, damaged archaeological sites, and palaeoseismic geological studies all show that the DSF has been active since the early-middle Miocene. Arid climate in the region made Lake Lisan stably stratified because the fresh water input floated whereas the dense saline bottom waters remained anoxic. Consequently the lake bottom was lifeless and therefore the fine seasonal mm-scale laminated deposits remained undisturbed. In terms of composition, the white layers are pure aragonite, while the intervening dark laminae contain tiny detrital

grains primarily of limestone, dolomite, minor quartz and feldspars (aeolian) together with rare lithoclasts of various types including basalt from the eastern shore of the present Dead Sea (Fig. 5a). The lighter-coloured aragonite-rich layers formed during arid (summer) conditions when there was little influx of clastic material. Conversely, the darker clay-rich layers reflect increased clastic input during wet (winter) periods. The lamination facilitates the recognition of even the slightest deformation, as demonstrated by sub-mm observations on seismites (Migowski et al., 2004).

3.3. Structures within the Lisan Formation

Deformation of distinct layers in the form of folds is very common in the Late Pleistocene Lisan Formation (Fig. 5a, b). El-Isa and Mustafa (1986) postulated that the folds formed when seismic waves deformed the sediments at the lakebed. The discovery of turbulent breccia layers abutting syndepositional faults (Marco and Agnon, 1995; Agnon et al., 2006) proved that the breccia layers are seismites, thus providing a palaeoseismic record spanning 70–15 Ka (Marco et al., 1996). Confirmation of these layers as seismites was found in the temporal correlation of Late Holocene breccias with historical earthquakes (Ken-Tor et al., 2001; Migowski et al., 2004). The deformation features, including asymmetric folds, typically appear in layers with widths varying from centimetres to metres and are enclosed between undeformed layers (Fig. 5a, b, c). The work of Heifetz et al. (2005) and its extension by Wetzler et al. (2009) suggests that the breccia layers are the final stage of

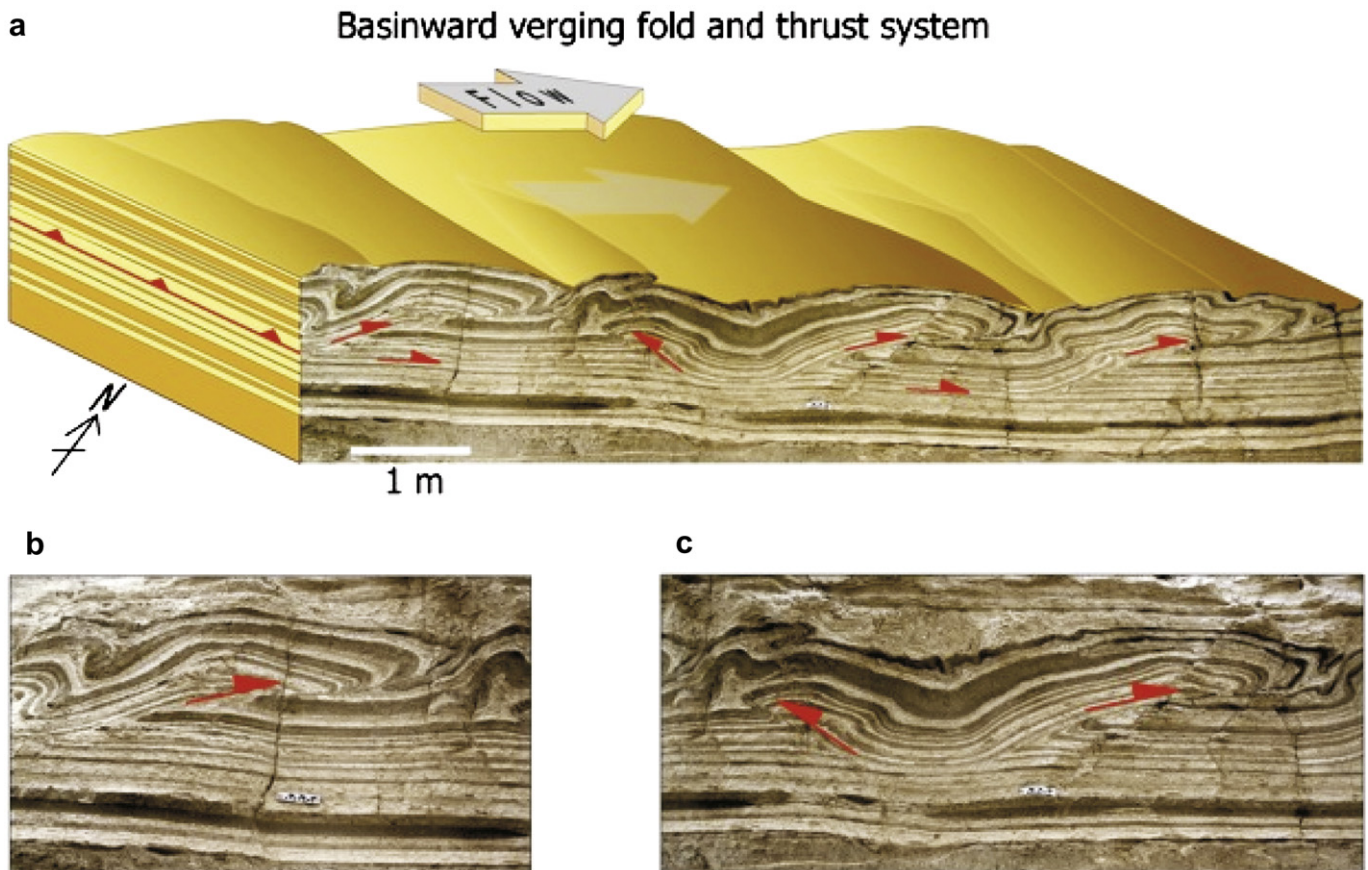


Fig. 7. Photograph and schematic interpretative top surface of a metre-scale fold and thrust system translating downslope towards the NE at Peratzim. The ~ 9 m section (a) comprises a thrust system that is underlain by an undeformed sequence. Backfolds are developed above the northeastern-most thrust ramp (above the tail of the thrust ramp arrow). Details of the left and central parts of the section are shown in b) and c) respectively. A typical thrust ramp is shown in b). Note the development of marked backthrusting in c) that tips out into a contractional fold to create an overall synformal geometry. Minor folds relating to secondary slumping verge down towards this trough during relaxation. Undeformed beds cap this slump (observed in c).

deformation which began as laminar moderate folds, evolved into billow-like asymmetric folds, then coherent vortices, and finally turbulent chaotic structures such as breccia. Our measurements of undisturbed bedding in the Lisan Formation show dips of less than 1° , which indicates stable conditions. Hence we assume that the folds were triggered by earthquake vibrations and that their geometry was dictated by the very subtle initial slopes.

4. Detailed observations of contractional and extensional slump geometries

4.1. Description of slump folds at Peratzim

Peratzim at the southern end of the Dead Sea (N $31^\circ 04' 49.6''$ E $35^\circ 21' 04.2''$) provides an exceptionally well-exposed case study section through slump geometries in the Lisan Formation (Fig. 4c). In the following sections, SW is on the left and NE is on the right of all photographs (unless stated otherwise), while the hammer (30 cm long), paper ruler (20 cm long) and coin (15 mm diameter) act as scales. Slump folds at Peratzim are typically <1 m wavelength and form in packages less than 1 m thick, although thrust sequences can be up to 2 m thick (Fig. 5a). Folds are upright to more typically recumbent with rounded rather than angular hinges (Fig. 5b). The aragonite-rich layers tend to be more competent and resistant to erosion as shown by buckle fold geometries with weaker mud-rich units simply flowing and “infilling” space around folds (Fig. 5b). Detailed structural analysis of a ~ 25 m long case study section reveals NW–SE trending gently plunging fold hinges (Fig. 6a–h). Fold hinges in this section are uniformly orientated suggesting only limited hinge rotation during slump translation, and no evidence for highly curvilinear folding that may complicate vergence and facing patterns (e.g. Alsop and Holdsworth, 2004a). Axial planes are SE-striking and typically dip gently towards the SW, although more steeply NE-dipping axial planes are also recorded (Fig. 6f, h). A minority of axial planes dip very gently towards the NE and are associated with back folding off the dominantly NE-verging fold and thrust system (Fig. 6a, b) (see Section 4.2 below). Steeper axial planes (thought to have been less rotated during progressive deformation) are typically considered as more reliable indicators of shearing and downslope directions (Strachan and Alsop, 2006; Lesemann et al., 2010). Axial planes that dip moderately to steeply SW ($>45^\circ$) trend on average 124° , suggesting that the palaeoslope direction would be towards 034° (see summary of methodology in Strachan and Alsop, 2006 and Debacker et al., 2009). Fold facing is typically up towards the NE, although upwards SW facing associated with backfolding is also observed (Fig. 6e, f). The general facing direction is towards 042°

broadly parallel to the assumed palaeoslope direction (Fig. 6). NW–SE striking thrust planes are gently SW-dipping, although more steeply NE-dipping “back thrusts” are also developed (Fig. 6a–d). Overall, the coherent and consistent fold and thrust system exposed at Peratzim is associated with NE-directed vergence (Fig. 6). Details of these fold and fault geometries are now explored in more detail.

4.2. Imbricates, back-thrusts and -folds within downslope verging thrust systems

Typical downslope verging thrusts are marked by bedding sub-parallel flats ($<1^\circ$ dip) and ramps with dips of $<30^\circ$ although these may be subsequently rotated to $>40^\circ$ due to back-steepening associated with piggyback thrusting (Figs. 6 and 7). Thrusts typically form imbricate fans as a) ramping thrusts fail to cut up and join an overlying roof thrust, b) ramps may cut to the lake floor and create topography that may influence sedimentation. Within slumps, back-thrusts/folds locally mark displacement in the upslope direction and although they have received little attention in the literature, their recognition is clearly crucial in interpreting palaeoslopes in ancient settings. Back thrusts typically form with ramps dipping at $<30^\circ$ in the downslope direction, although it should be noted that they can be significantly steeper ($>65^\circ$) than adjacent forethrusts (Fig. 6c, d). This may reflect subsequent steepening due to additional contraction during slump cessation. Layers of weak mud along which thrust flats propagate also act as detachments for back thrusts that typically root smoothly downwards. The overall geometries and sequences are very similar to those formed in sandbox experiments above a weak basal polymer layer (Fig. 8). Displacement on back thrusts diminishes upwards (as with forethrusts), and may tip out into backfolds (Fig. 7c). Small-scale back thrusts may locally develop within the hinges of downslope verging slump folds, although they simply represent a mechanism to accommodate local shortening associated with the folding process. Similar structures have been observed in analogue models (e.g. Noble and Dixon, 2011). Minor back thrusts associated with backfolds may also develop directly above a downslope verging thrust ramp (Fig. 7a, c).

Back-folding is also interpreted to develop in response to back-steepening of folds and thrusts during downslope propagating piggyback thrusting. In this scenario, folds and thrusts are seen to be progressively back-rotated until folds verging back upslope (i.e. in the opposite direction to the original thrust displacement) are formed in the most back-steepened and unstable thrust imbricate (Fig. 9a). Due to the layer-cake stratigraphy and constant fold/thrust wavelength, it appears that the critical angle for this gravity-driven

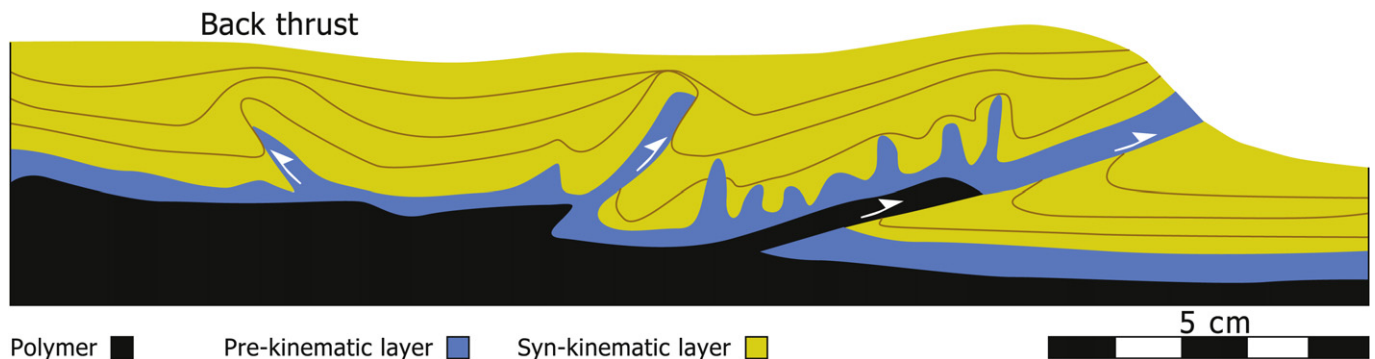


Fig. 8. Line drawing of an analogue experiment (courtesy of Xavier Fort) showing pre- and syn-kinematic sand layers deposited above a weak basal polymer layer. The section displays thrusting which affects younger syn-kinematic layers towards the right in a piggyback sequence. Early upright folds in the pre-kinematic layer are carried on the hangingwall of thrusts which root directly into the polymer, and which cause a slight back steepening of the folds. Steep back thrusts also root directly into the polymer.

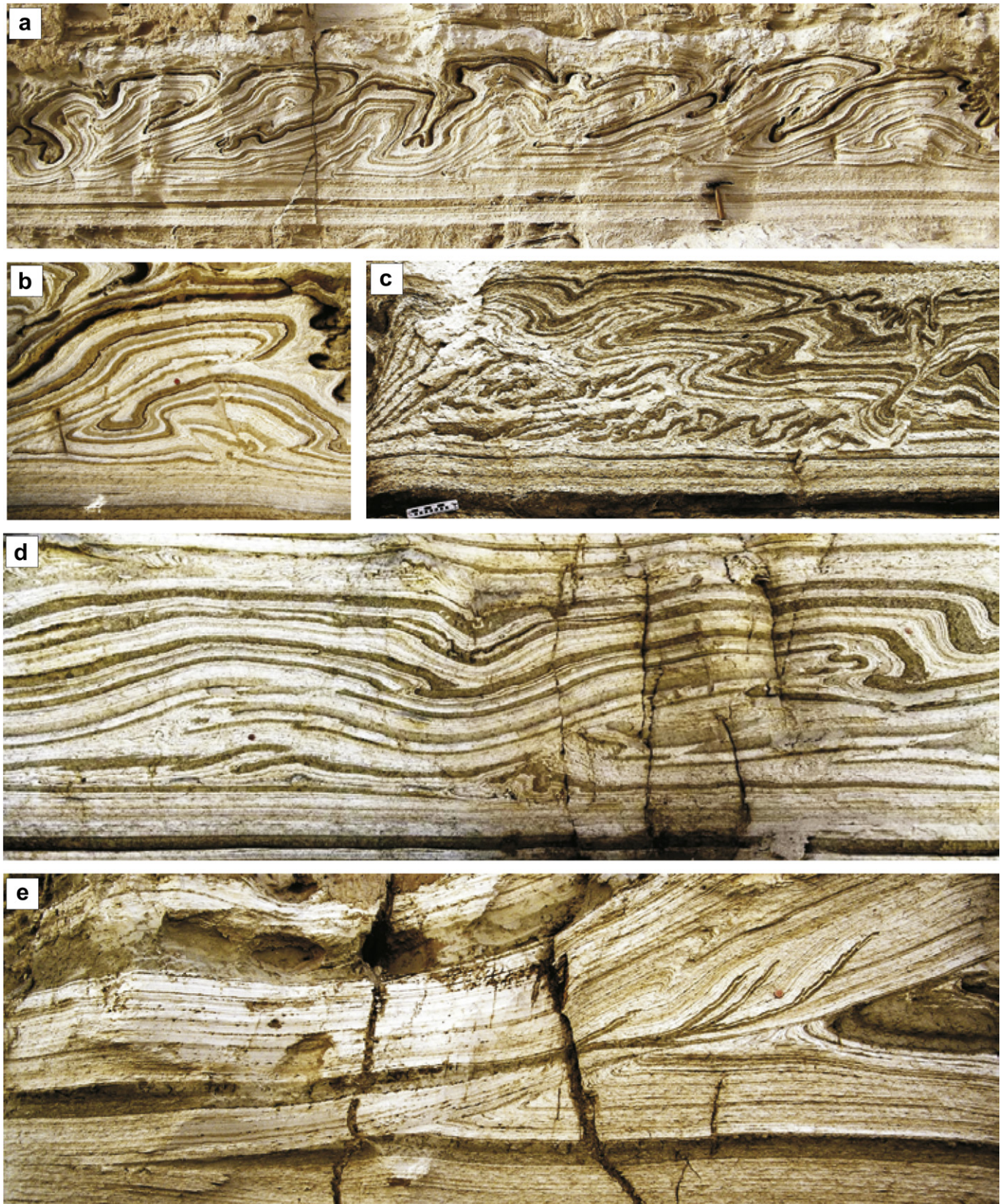


Fig. 9. Collection of photos showing brittle thrust imbricate structures at Peratzim. a) Slumped sequence showing backfolds developing off thrust and fold imbricates associated with NE-directed slumping. Note how backfolds form off every 3rd imbricate after it has been sufficiently back-steepened during piggyback thrusting to become unstable. b) Details of the NE-end (right) of section a). Back thrusts dipping at $>45^\circ$ towards the NE are developed within the cores of NE-vergent slump folds. c) Details of intense NE-directed imbrication and thickening of the lower part of a slump sequence, which is accommodated in the upper (more mud-rich) parts by folding. d) Details of a thrust-dominated slump associated with NE-directed slumping. Thrusts typically die out into folds in the upper parts of the slump marked by more pronounced mud-rich layers. e) Metre-scale thrust that cuts across and displaces the lower mud-rich marker. An earlier thrust is located within this mud-rich marker, and results in imbrication of the upper part of the mud layer (by coin). This early thrust is cut across by the lower thrust indicating a piggyback sequence of thrusting.

back folding is reached where thrusts have been back steepened to $\sim 40^\circ$ typically in every third imbricate of a piggyback sequence (Figs. 9a, b, 10).

In detail, intense localised imbrication and thickening of the lower part of a slump sequence may be accommodated in the upper (more mud-rich) parts by folding (Fig. 9c, d). Pronounced back-steepening in some instances (e.g. Fig. 9c) supports a piggyback sequence of deformation. Piggyback thrusting is also confirmed by thrust cut-off relationships, where overlying thrusts are cut by younger thrusts in their footwall (Fig. 9e). Back-steepened thrusts associated with piggyback thrusting display consistent small, steep thrusts towards the rear of the thrust slice (Fig. 10). These small secondary thrusts branch from the underlying flat at a similar position as the larger thrusts, and are markedly back rotated during thrusting, indicating that they formed sequentially during overall piggyback thrusting. (Fig. 10). Similar piggyback thrust systems have recently been produced in analogue experiments by Noble and Dixon (2011).

4.3. Slope-normal extensional fault geometries

Syn-slumping extensional faults are typically considered to form at the head of the slump and form listric geometries that root downwards into an underlying detachment (Farrell, 1984) (Fig. 1). They are normally considered to form at high angles to the slump direction, although may display downslope concavity in map view as they curve into strike-slip systems at the margins of slumps

(Fig. 1). In the present study, extensional faults are seen to be moderately-steeply (40° – 60°) dipping towards the east (e.g. Fig. 11a–g). Pre-existing slumped horizons may be extensionally offset by these faults, indicating that slumped units may be reworked by younger faults, which are overlain by undeformed horizontal beds (Fig. 11a, b). Beds in the hangingwall of normal faults may be upturned to dips $>40^\circ$ which results in localised secondary slumping down the fault scarp (Fig. 11e). Coupled with this secondary slumping, significant thickening and growth of strata in the hangingwall of normal faults confirms that the fault displaced the lake floor and influenced sedimentation (Fig. 11c, d, e). Individual fault scarps may be marked by several fault strands, with the hangingwall growth strata comprising mud-rich breccia units perhaps representing a turbidity flow generated during the same event (Fig. 11c, d). Downslope verging slumps above the growth strata are cut by the continuation of this fault, suggesting that it has been reactivated on a number of occasions and continued to operate over a period of time (Fig. 11c, d).

In addition to the extensional faults described above that locally effect sedimentation patterns, a series of small scale normal faults, frequently with a domino geometry, are locally developed within individual slump systems (Fig. 11f, g). In some cases these can be directly linked to the downslope vergence of adjacent folds (Fig. 11f). In other cases the extensional faults form part of a detachment system where steeper normal faults that displace mud-rich units flatten downwards into bedding sub-parallel detachments (Fig. 11g). The steeper fault segments faults are

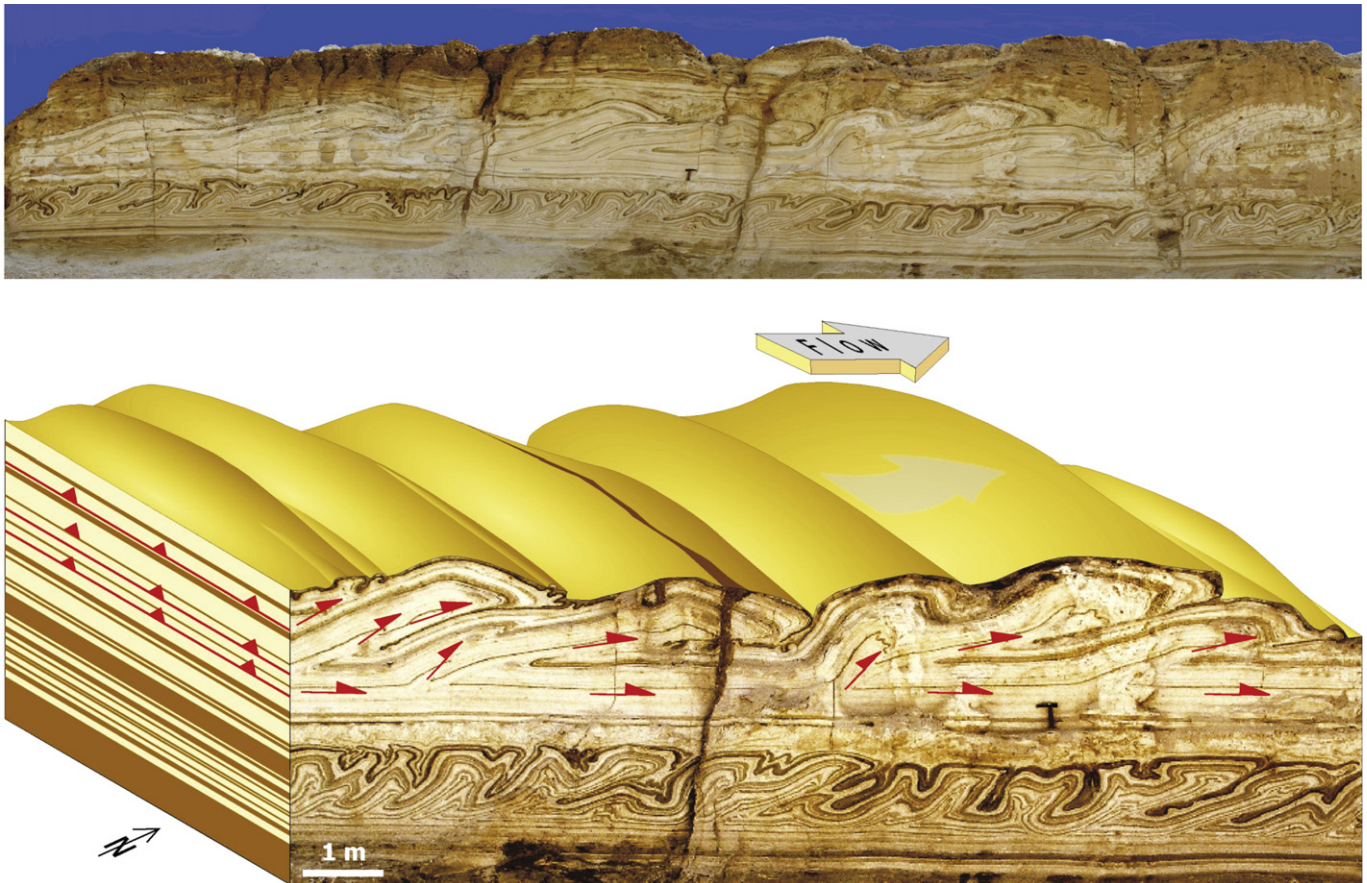


Fig. 10. The photograph (above) shows part of a ~ 25 m long wadi section cutting through Lisan Marls at Peratzim. Spectacular slump folds and a thrust imbricate fan are developed on a metre scale and display vergence towards the NE and the Dead Sea Basin. Note the undeformed beds both beneath and above each deformed unit, together with later sedimentary injections which cut the folds. The upper sequence of NE-directed thrusts is marked on the right by a recumbent isoclinal fold, suggesting that this may be close to the leading edge at the toe of the slump sheet. The lower photograph and 3-D interpreted top surface represent the central portion of the overlying photo. Steep thrusts are developed close to where imbricates branch off the floor thrust, indicating back-steepening and a piggyback sequence of thrusting.

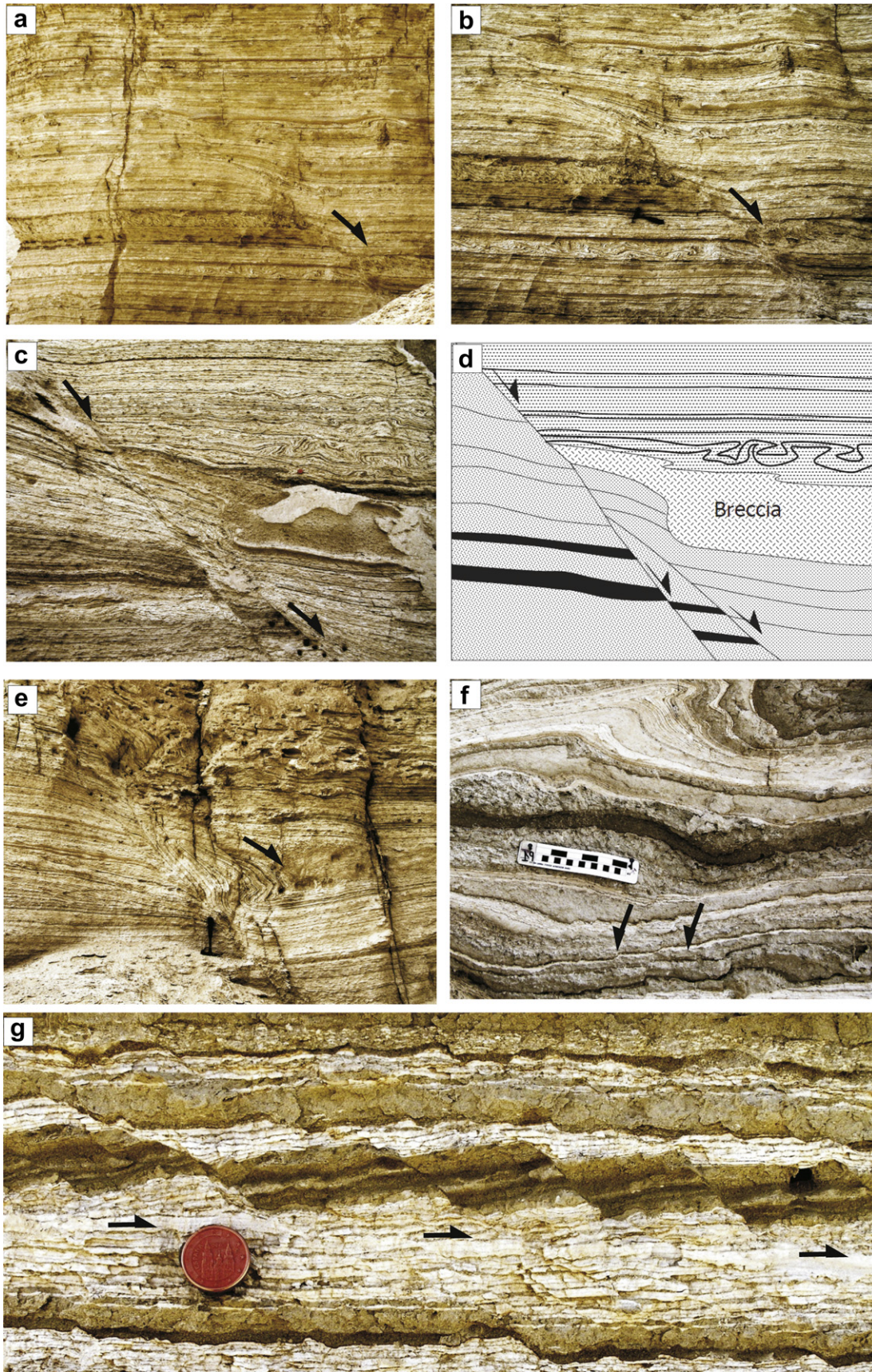


Fig. 11. Normal faults associated with slumping from Masada (a–e) and Peratzim (f–g). a) and b) Moderately dipping ($\sim 40^\circ$) extensional fault cutting sub-horizontal beds and slumped units and displaying top down to the East movement. Displacement across the fault is greatest at the base (~ 1 m) and diminishes upwards, until the fault plane is overlain by undeformed strata, some of which exhibit a slight thickening on the downthrown side. Small slump folds also develop local onlap relationships above their crests. Photograph

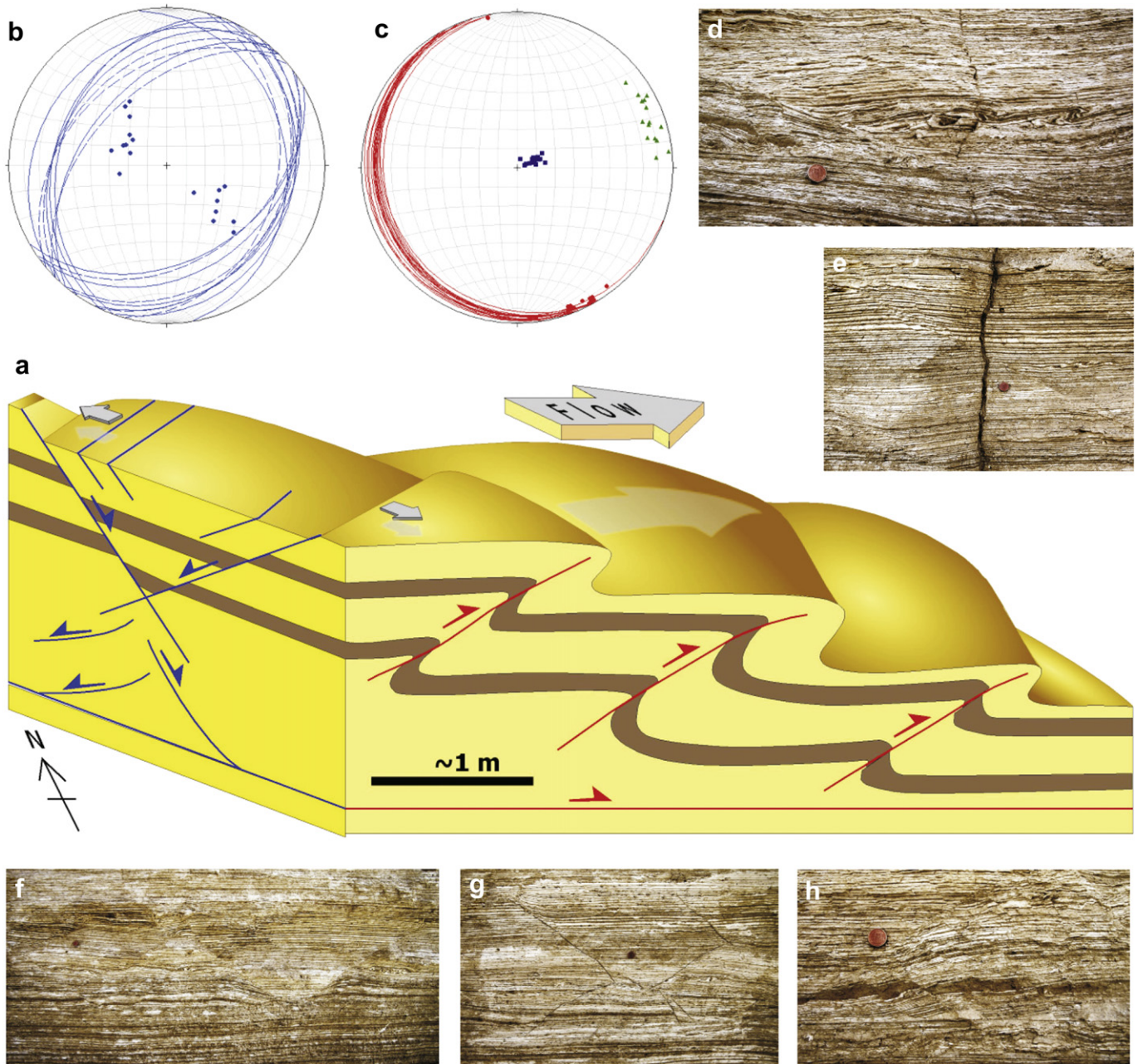


Fig. 12. a) Schematic cartoon illustrating contractional folds and thrusts (shown in red) associated with ENE-directed slumping and flow at Masada (refer to Fig. 4 for location). Conjugate extensional faults (shown in blue) are developed slightly counterclockwise of the main slump direction and suggest that extension at a high angle to flow occurred during slumping (shown by small arrows). b) Stereonet showing syn-sedimentary extensional faults (in blue) as great circles and poles to great circles ($N = 18$). The NW-dipping (mean $038/45\text{NW}$) and SE-dipping (mean $032/28\text{SE}$) extensional faults form a conjugate system with an intersection at $2/035$. c) Stereonet of data from the same section showing SE-trending fold hinges (red circles), SW dipping axial planes (blue squares and red great circles) and ENE-trending facing directions (green triangles). Fold data ($N = 16$) suggests slumping towards the ENE. d) Extensional faults and slump folds verging towards the ENE. e) Syn-sedimentary extensional faults that result in thickening of overlying layers, and which are cut by sedimentary injections. f) Syn-sedimentary conjugate extensional fault system that is overlain by an undeformed horizontal sequence. The section is NNW-SSE trending and corresponds to the end face of the schematic block diagram. g) Interaction of conjugate extensional faults that result in thickening of overlying layers. h) Listric extensional faults that cause rotation of minor fault blocks and flatten markedly into an underlying sub-horizontal planar detachment. Other faults are more planar and appear to detach onto a weak mud-rich layer.

(c) and interpreted line drawing (d) of an extensional fault system dipping at 50° with marked downthrow towards the east. Hangingwall growth strata comprise a mud-rich breccia with the top of this unit marked by downslope verging slumps (left of coin). e) Pronounced normal fault marked by dramatic upturn of hangingwall strata. This upturn of beds to dips $>40^\circ$ is inherently unstable and resulted in localised secondary slumping down the fault scarp. f) Steep ($\sim 70^\circ$) SW-dipping domino faults developed in mud-rich unit at Peratzim. Although each domino is marked by SW-down movement, the overall sense of domino sliding is associated with top to the NE movement, in agreement with vergence of the overlying slump fold. g) A series of pronounced cm-scale normal faults that clearly offset a mud-rich layer (centre) resulting in local back-rotation of the bedding. The lack of clear cross cutting high-angle faults in the aragonite-rich layer suggests that extensional deformation becomes bedding-parallel. A bedding sub-parallel extensional detachment (marked by black shear arrows) is developed directly above the 15 mm coin and is marked by a lighter-coloured band that transects bedding laminations.

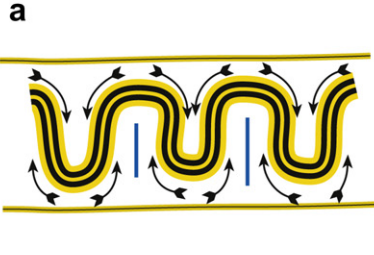
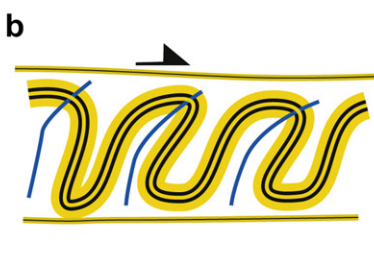
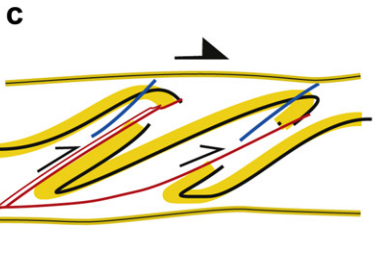
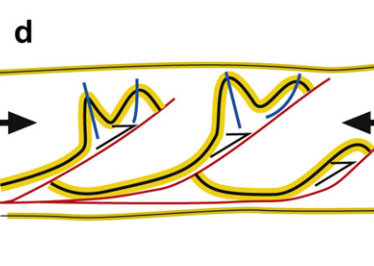
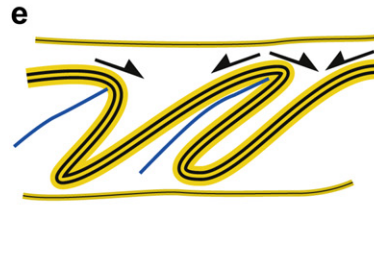
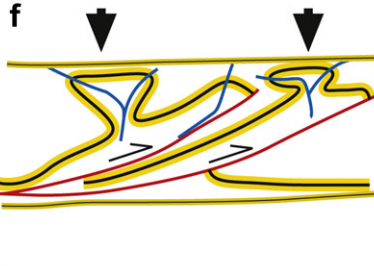
| | | | |
|-------------|---|---|--|
| Initiation | <p>Coaxial-dominated vertical movement</p>  | Density-driven fold initiation and/or horizontal shortening |  |
| Translation | <p>Non-coaxial-dominated down-slope movement</p>  | Non-coaxial gravity-driven amplification of folds |  |
| | <p>Continued non-coaxial gravity-driven amplification of folds and failure of lower fold limbs</p>  | Continued non-coaxial gravity-driven amplification of folds and failure of lower fold limbs |  |
| Cessation | <p>Horizontal shortening</p>  | Contraction-driven fold growth off thrustured folds during lock-up of slump |  |
| Relaxation | <p>Non-coaxial-dominated horizontal movement</p>  | Small-scale secondary slumping off the crests and toward synformal troughs of earlier folds |  |
| Compaction | <p>Vertical shortening</p>  | Vertical gravity-driven "flattening" of structures leading to mushroom folds |  |

Fig. 13. Schematic line drawings and photographic examples (from Peratzim) of structures generated during slump sheet initiation (a), translation (b, c), cessation (d), relaxation (e) and compaction (f). Folded beds are shown in yellow, while axial planes (blue) and thrusts (red) are also highlighted together with possible deformation styles. Not all slump sheets will show the full range and evolution of structures depicted here. Northeast is on the right of photographs.

associated with local thickening and thinning of the aragonite-rich layers suggesting a degree of plastic deformation (Fig. 11g).

4.4. Slope-parallel extensional fault geometries

In addition to the classical extensional faults that form at high angles to the downslope direction described above, a series of extensional faults that form a conjugate system with a mean acute angle of 63° and are oblique or sub-parallel to the downslope direction has also been identified in one case study area at Masada (Fig. 12 a–h). The strike of the conjugate fault system is marginally anticlockwise (trending $\sim 035^\circ$) of the folds and thrusts marking the downslope slump direction (trending $\sim 066^\circ$), and suggests that slumped sheets not only underwent typical downslope extension, but also lateral spreading along the strike of the palaeoslope (Fig. 12a, b, c). Thin (<5 cm thick) folded horizons may themselves be cut by the extensional faults, indicating that larger scale slumps may rework the small earlier slumps (Fig. 12d). These faults form part of metric-scale systems associated with contractional folds that are capped by overlying undeformed sediment layers, thus confirming the syn-slump nature of these faults (Fig. 12d, e). The extensional faults are themselves cut by syn-sedimentary injections that may display slight deviation directly beneath the fault plane (perhaps suggesting that upward injection has been hampered by faulted sediment) (Fig. 12e). Conjugate faults may display listric geometries as they flatten into underlying detachments (along mud-rich layers), which causes the overlying sediment packages to be rotated by up to 40° (Fig. 12f, g, h). The consequence of the observations presented above is that extension

(and a degree of contraction) may take place in the flow normal (i.e. strike-parallel) plane. The implication is that slump sheets may not necessarily be treated as plane strain systems and are likely to be associated with significant out-of-plane movement, as originally suggested for flow perturbation folds by Coward and Potts (1983) and Ridley (1986).

5. Structural evolution of the Lisan slump fold system

Farrell (1984) suggested that slump systems may be divided into an initial phase of development, followed by translation and a termination or “cessation” phase. Although it should be stressed at the outset that this general scheme is based on interpretational models, it does provide a useful framework with which to describe the Dead Sea slumps and has therefore been expanded and refined here (Fig. 13).

5.1. Slump initiation (Fig. 13a)

Initiation of slump movement may be triggered by a variety of factors that create instabilities and have been recently summarised by Gilbert et al. (2005). These mechanisms include the following.

5.1.1. Instabilities associated with sediment loading

Rapid sedimentation may encourage slumping by dramatically increasing the sediment load. In addition, rapid sedimentation may trap water between grains thereby increasing pore fluid pressure and effectively weakening sediments. In the case of the Lisan Formation, the varve-like nature of the sediments reveals

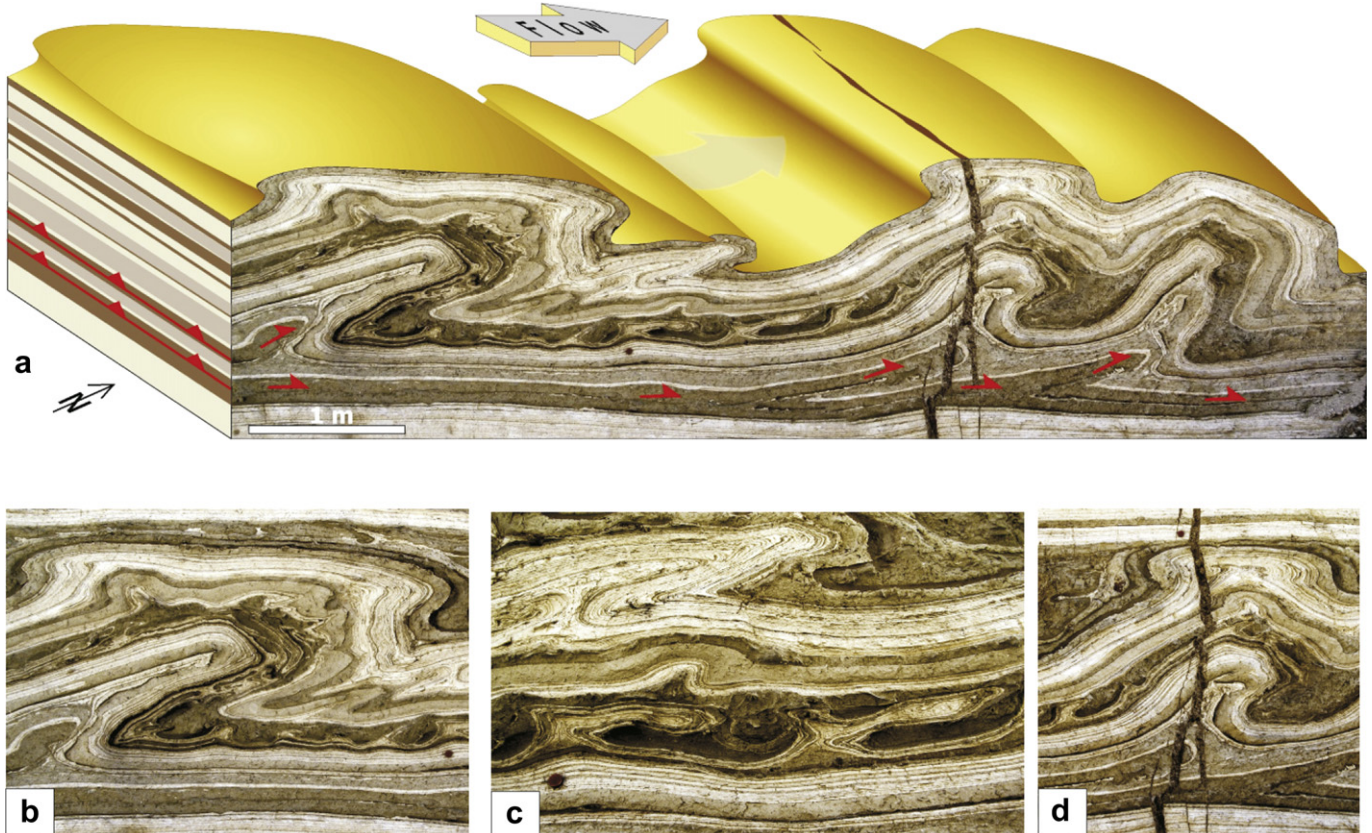
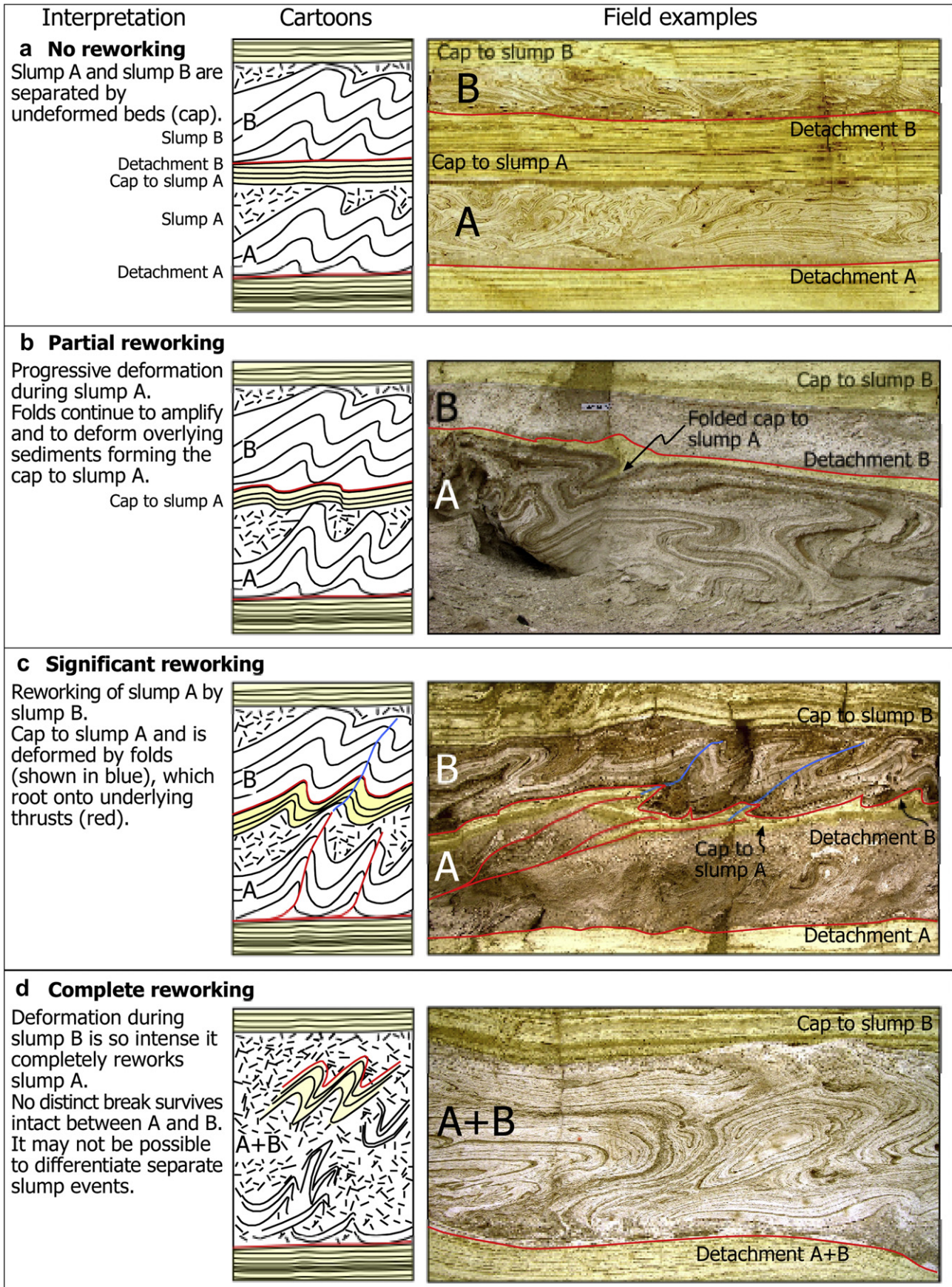


Fig. 14. a) Photograph and schematic interpretative top surface of a metre-scale fold and thrust system translating downslope towards the NNE at Peratzim. The ~ 7 m section shows thrusts verging towards the NNE (b), within the darker mud-rich layer, minor folds are sheared over and attenuated during translation of the thrust (c). These minor folds are refolded around the larger thrusts thus providing a relative structural chronology (b, c). d) Upright mushroom-shaped folds with sub-horizontal crenulations (in the hinge below the coin) grow off the thrusts during later cessation and relaxation. The deformed sequence is cut by a sedimentary injection which displays consistent right-stepping up through the sequence.



a relatively slow and stable sedimentary input that would not encourage slump initiation via overloading.

5.1.2. Instabilities associated with over-steepening

Regional tectonics may result in tilting of fault blocks, thereby encouraging slumping of sediments off local fault block “highs”. However, the Lisan Formation, although located in a tectonically active area along the Dead Sea fault system, does not display steep dips with the average dip of the Lisan Formation being $<1^\circ$. This mechanism can therefore be effectively ruled out in this case study.

5.1.3. Instabilities associated with seismicity

Regional tectonics associated with seismicity triggers shaking that destabilises water-rich sediments leading to slumping. There is abundant evidence of long-lived seismicity along the Dead Sea fault system (see Marco et al., 1996) and we therefore consider this the likely trigger for slumping within the Lisan Formation

Based on hypothetical dislocation models, Farrell (1984) suggested that the initiation of slumping by a seismic event typically occurs at a single point of failure and may be achieved by a coaxial pure-shear component of shortening, which generates upright buckle folds leading to a parallel fold style (Woodcock 1976a, b; Farrell, 1984) (Fig. 13a). In the example shown (Fig. 13a), the upright folds must be underlain by a bedding-parallel detachment which separates the slumped sequence from the underlying and undeformed beds. Vertical movement of sediment during horizontal shortening may also be achieved by density-driven folding along contacts of marked contrast (Fig. 13a) (see Section 7.2). This upright “billow” style of folding is restricted to thicker mud-rich horizons that may trap significant volumes of water within them during deposition. This would encourage such density-driven folding, possibly associated with Rayleigh-Taylor or Kelvin Helmholtz instabilities (see Section 7.2).

5.2. Slump translation – early phase (Fig. 13b)

The translation phase is marked by downslope movement of sediment associated with non-coaxial dominated deformation (Fig. 13b). The role of non-coaxial deformation has been previously recognised by Woodcock (1976a, b) and Farrell (1984) and results in gravity-driven amplification of the pre-existing folds (Fig. 13b). Thus, upright folds created during initiation of the slump are markedly sheared over, and may undergo significant growth and increase in amplitude (Fig. 14a, b, c). Increase in fold amplitude must have occurred when folds were already in a sub-recumbent attitude as the surrounding mud-rich layer is not thick enough to support upright folds of that “height” (Fig. 14c).

5.3. Slump translation – late phase (Fig. 13c)

Continued non-coaxial dominated downslope deformation results in amplification of folds and may ultimately result in fold limb failure (Fig. 13c). This is associated with the development of downslope verging thrusts (Fig. 14a–d). Sub-recumbent folds generated during the earlier translation phase (Section 5.2. above) are refolded around these downslope verging thrusts and folds to create classic refold patterns and thereby provide a clear relative chronology.

5.4. Slump cessation (Fig. 13d)

Cessation of the slump movement may occur first at either the trailing edge (head) or leading edge (toe). If it develops at the head (perhaps due to water escape locking the normal fault) then extensional strain propagates downslope. We see only limited evidence at Peratzim of late normal faults cutting slumps that could be attributed to such a mechanism. Conversely, if the toe locks up first then a contractional wave of deformation propagates back up the slump resulting in shortening of existing structures and possible development of new folds and thrusts (Fig. 13d). Contraction-driven fold growth due to this horizontal shortening leads to the development of upright folds growing off pre-existing thrusts and folds (Fig. 14).

5.5. Slump relaxation (Fig. 13e)

The structures generated during initial slump translation and cessation may subsequently undergo a phase of gravity-driven relaxation associated with secondary slumping off earlier structural highs (Fig. 13e). The direction of secondary slumping is governed by local culminations and is consistently towards the synformal troughs of earlier folds. Secondary slump systems may thus display reversals in vergence around earlier highs (Fig. 13e) which has the effect of a) thinning weak units over the crests of local highs; b) structurally thickening weak units within the troughs, c) locally creating secondary slump folds that verge up the regional palaeoslope (Fig. 13e).

5.6. Slump compaction (Fig. 13f)

Flat lying and late stage (“F2”) crenulations developed on the upright limbs of earlier F1 slump folds were interpreted by Farrell and Eaton (1988) as representing a compaction-generated fabric. Although Farrell and Eaton (1988) observed pyritically folded sandstone injections related to this 30–40% flattening, the case study from the Dead Sea shows no such compaction of the vertical sedimentary injections which retain pristine intrusive geometries (e.g. Figs. 5a, b, c and 14). This may suggest that the sedimentary injections are a relatively late-stage phenomena relating to strain associated with emplacement of the Mount Sedom salt diapir (Marco et al., 2002). A sub-horizontal crenulation fabric is however locally developed on the steep limbs of early folds (Fig. 14d). These minor folds do not verge towards the larger upright folds and are therefore not parasitic to these folds. They have simply been superimposed on the pre-existing upright folds. Vertical shortening during compaction leads to a slight flattening of upright structures and may amplify the “mushroom” geometries of some folds created during the cessation and relaxation of slump sheets (Figs. 13d, e, f and 14b, d). A lack of pervasive sub-horizontal compaction fabrics may reflect the fact that a) many slump folds are recumbent with bedding on sub-horizontal long limbs already parallel to compactional strain, b) slumps may be cohesive and semi consolidated at the time of compaction and therefore not susceptible to fabric development. Within the present case study, normal faults and thrust faults retain typical dips of 60° and 30° respectively suggesting that compaction has not significantly reduced these angles (see Section 4.2 above). These observations suggest that

Fig. 15. Schematic cartoons and field examples from Peratzim of various degrees of reworking of an original slump (A) by a subsequent slump event (B). a) Where no reworking of slumps occurs, slump A is underlain by detachment A and separated from the overlying slump B by an undeformed sedimentary cap. b) Where partial reworking occurs, the cap to A and detachment B are gently folded and deformed. c) Significant reworking of underlying slump A by structures associated with slump B occurs. Thrusts developed in slump A cut the overlying Cap to A and generate folds in slump B which root onto the underlying thrusts. d) Complete reworking of the older slump A by the younger slump B resulting in the distinct break between the two events being completely destroyed and overprinted.

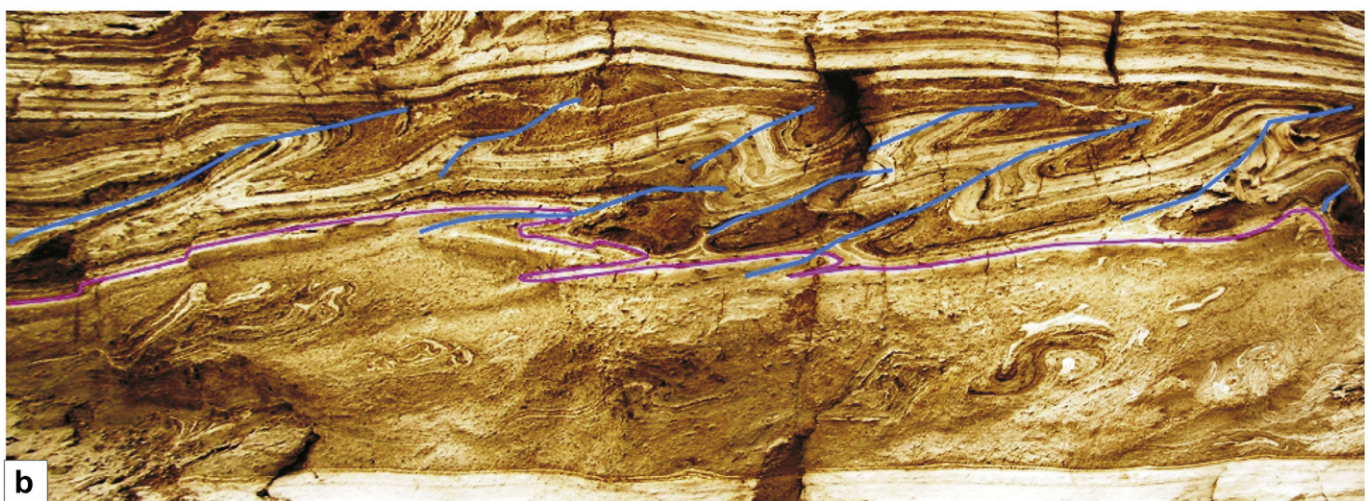
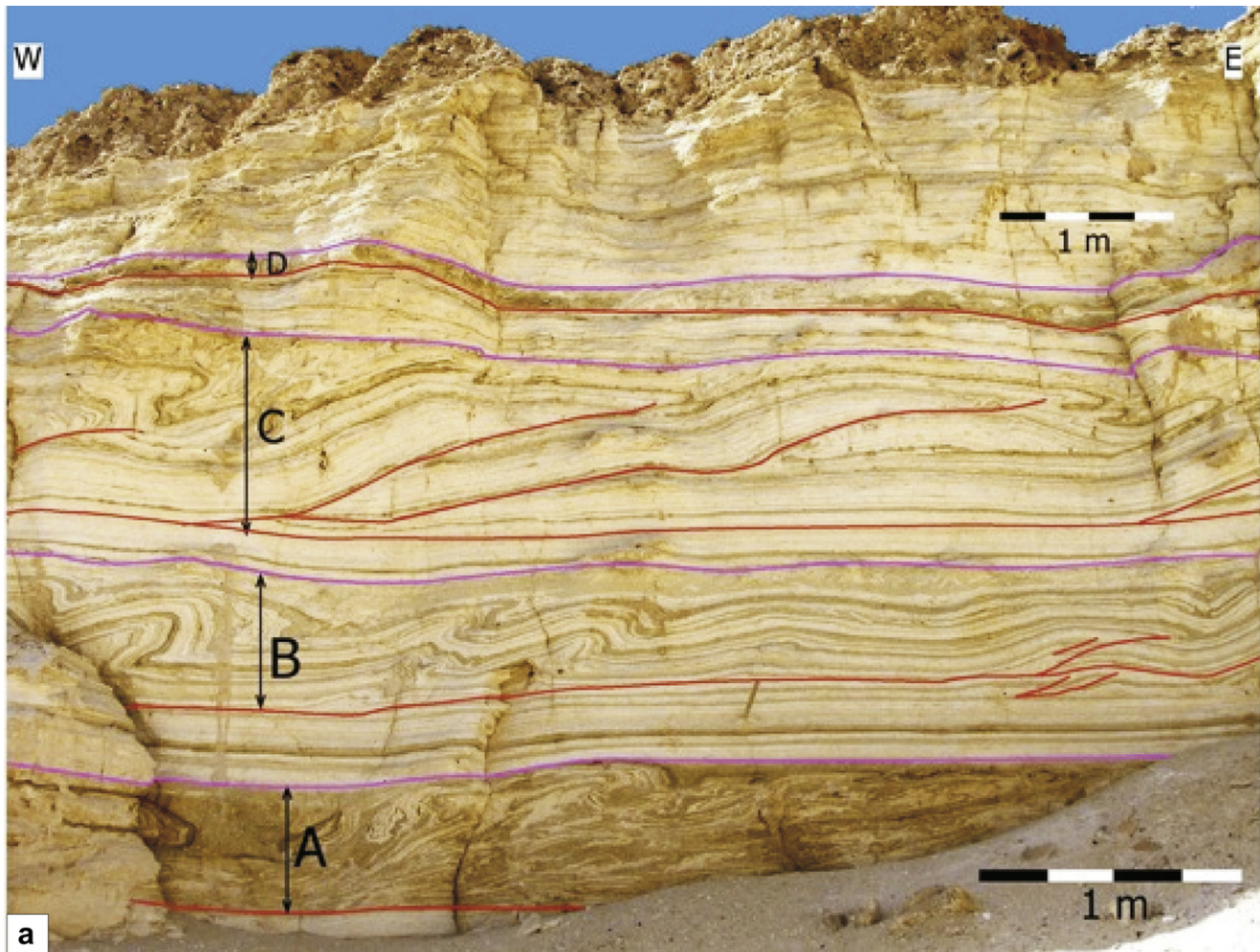


Fig. 16. a) This photo from Peratzim highlights 4 distinct slump sequences (labelled A–D) that are separated from one another by undeformed horizontal beds that “cap” each slump event. Slump A at the base of the section displays the most deformed and chaotic sediments, Slump B is marked by distinct NE-verging folds and subordinate thrusts, Slump C displays classic imbricate fan thrust geometries with steepening of thrust planes towards the west suggesting an NE-directed piggyback sequence of propagation, while slump D forms the thinnest slumped sequence and youngest of the events. b) Reworking of structures in a lower slump system by those associated with an upper slump at Peratzim. The breccia layer below the magenta line was reworked by the event that folded the overlying slump layer. Note how the axial planes of folds (shown in blue) may be traced across the two sequences.

compaction does not typically play a significant role in altering structural geometries generated during the earlier slumping.

6. Interaction and reworking during multiple slump events

6.1. Controls on slumped unit thickness

As shown by a number of authors including Marco et al. (1996) and Wetzler et al. (2010), the thickness of a slumped unit depends on a variety of factors including:

(i) The local intensity of the seismic event, which is dependent on the magnitude and proximity of the triggering earthquake, and the mechanical properties of the sediment together with the attenuation of seismic waves. (ii) The gradient of the slope. (iii) The composition and texture of sediments, which includes factors such as mineralogy, grain size, density distribution, viscosity and porosity. (iv) The height and composition of the water column, including the density of brine versus sediments. (v) The local sedimentation rate and how rapidly pore water is expelled from the sediment. (vi) The seismic recurrence interval as it is more difficult to shake water out of sediments when this has already been done once.

In practice, the major controls on the thickness of slumped units largely reflect a balance between sedimentation rates versus recurrence intervals. When sedimentation rates greatly exceed recurrence intervals, then thicker slumped units typically result, whereas more frequent recurrence intervals and/or slower sedimentation rates tend to produce thinner slumped units. In addition, small slope gradients ($<1^\circ$) may require larger intensity events to initially trigger slumping, and these being less frequent, may therefore affect thicker accumulations of sediment and hence generate thicker slumped units.

6.2. Distinguishing reworking of slumped units by multiple events

The ability to distinguish structures created during a single slump event from those generated during multiple reworking episodes is crucial if structures are to be correctly interpreted and histories revealed. Structural linkages across slumped units are examined, and we describe examples which for the first time provide direct evidence for multiple reworking of slump sheets.

6.2.1. No reworking of a slumped unit

Individual slumped units are normally readily identified as they are capped by an overlying sequence of undeformed sediments i.e. slump A will be overlain by an undeformed cap to slump A (Fig. 15a). In addition the base of a slumped unit is frequently (although not exclusively) marked by a sub-horizontal detachment which separates the slumped unit from the underlying undeformed sequence i.e. slump unit A will be underlain by detachment A (Fig. 15a). When packages of sediment between the two slumped units remain entirely undeformed, then clearly there has been no reworking of the older slump horizon (A) by the overlying younger slump sequence (B) (Fig. 15a). In this case each slumped horizon will therefore represent a separate seismic event with no “structural linkage” between the two (Fig. 16a). New detachment surfaces will tend to form in the beds deposited above the previous slump horizon, as these are flat, “layer-cake” and heterogeneous thereby providing easy-slip surfaces. The old, folded and convolute slump horizon is inherently more difficult for new detachments to propagate through, and in addition may have become partially lithified if the seismic recurrence interval is long or sedimentation is rapid.

6.2.2. Partial reworking of a slumped unit

Partial reworking of an older slumped unit (A) may be recognised if the overlying cap to slump A is weakly deformed by folds

that are also seen to fold the detachment to slump B (Fig. 15b). Structures in slump A are in this case considered to continue to develop and progressively amplify after deposition of the cap to slump A and slump B (Fig. 15b). This form of partial reworking in slump A may be triggered by seismicity associated with a younger slump (B), although some gentle amplification of folds may occur during late-stage relaxation and compaction. Fabrics in breccia at the top of slump A may be gently warped by this later stage folding.

6.2.3. Significant reworking of a slumped unit

Significant reworking of an older slumped unit (A) may be recognised if the overlying cap to slump A is markedly deformed by folds that are also seen to fold the detachment to slump B (Figs. 15c and 16b). Folds in slump B may root directly into thrusts within slump A, thereby confirming a direct structural linkage between the two (A + B) slumped horizons, although they are still clearly discernible as two separate events (Fig. 15c). These structures are then overlain by undeformed sediments forming the cap to slump B, thereby confirming their belonging to slump B. Fabrics in breccia at the top of slump A may be folded by this later stage (B) folding.

6.2.4. Complete reworking of a slumped unit

Complete reworking of an older slump (A) by a younger slump (B) may result in the distinct stratigraphic break between the two events (cap to slump A) being completely overprinted and destroyed (Fig. 15d). The lowermost detachment therefore represents a composite structure relating to both slumps A and B (Fig. 15d). The critical lack of an intervening sedimentary cap between A and B means that it may not be possible to categorically differentiate the two discrete slump events which have become indistinguishable.

7. Discussion

7.1. Why do different fold and thrust styles develop in adjacent layers?

Slumped units contain a combination of folds and discrete thrust faults (Fig. 17a). This variation may be a consequence of a number of factors including the following.

7.1.1. Variable strain rates

Folding may be considered representative of relatively low rates of applied shear strain (Marrett and Peacock, 1999), while faster strain rates may encourage more discrete thrusts to form. In the present study it would appear that as some thrusts and folds form in the same layers as part of the same slump event, then this may not be the dominant controlling factor.

7.1.2. Variable displacement gradients

Displacement within the slump may theoretically increase up or down the deforming sequence depending on the type of flow and mechanical nature of the sediments being deformed (including variable pore fluid pressures). In the present study, there is no shear criteria or other evidence that lower parts of the slump moved more rapidly or further than the upper parts, suggesting that this may not be the dominant controlling factor.

7.1.3. Variable thickness of the slumped unit

The thickness of individual slumped sheets could be anticipated to influence the nature of fold or thrust deformation, as thicker slumped sequences may be triggered by larger seismic events which would encourage greater deformation and thrusting. However, in the present study, there is no such correlation between thickness of slumped unit and fold/thrust mechanism of

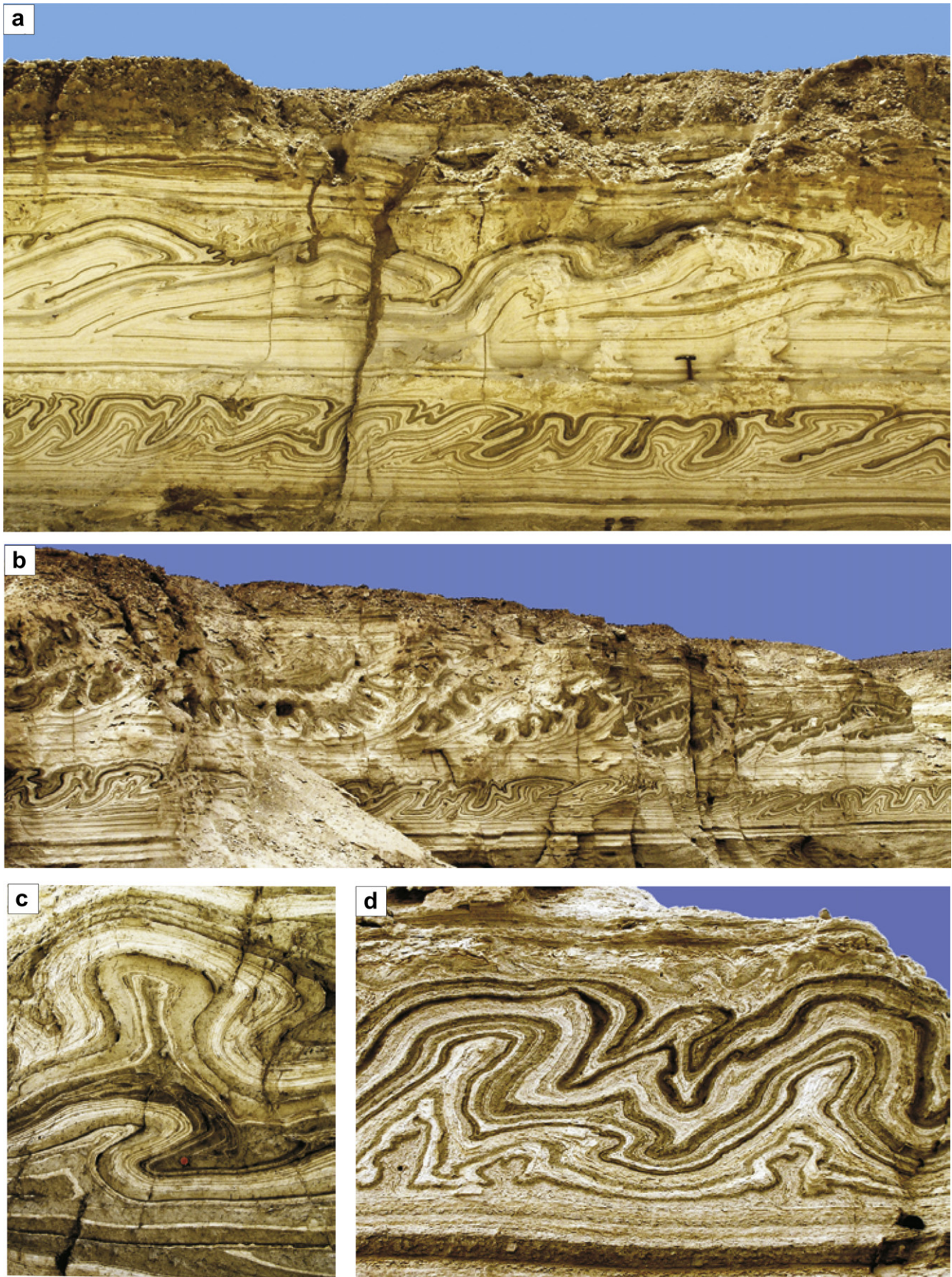


Fig. 17. a) Photograph of a metre-scale fold and thrust system translating downslope towards the NNE at Peratzim. The ~14 m section comprises a lower folded sequence forming slump 1, that is separated from the overlying thrust system (slump 2) by undeformed sediments. Both folds and thrusts display distinct vergence towards the NNE and the assumed

deformation suggesting that this may not be the dominant controlling factor.

7.1.4. Variable lithology

Different lithologies may display different mechanical behaviours, with folding tending to develop in lithologies more susceptible to plastic deformation, while thrusts may form in lithologies more prone to brittle styles of deformation. In the present case study, folding appears to develop more in mud-rich sediments, and thrusting in more aragonite-rich units (e.g. Fig. 17a). Mud-rich units are considered weaker as they typically thicken within the hinges of folds, and may also infill the central cores of detachment folds above the decollement layer.

This observation suggests that lithology may play an important role in the style of deformation, and is also supported by recent analogue experiments by Noble and Dixon (2011) which demonstrate that competent units separated by thin incompetent horizons are more likely to have strain accommodated on thrust ramps. Similar lithological controls on styles of deformation have been noted elsewhere and on different scales. Within salt tectonics, a lack of weak salt that would normally infill the cores of detachment folds has led to shortening being mostly accommodated by reverse faults (Stewart and Clark, 1999; Rowen et al., 2004).

7.2. Why do distinct progressive deformation sequences develop?

The sequence of deformation within many slump systems is difficult to unravel due to a) incomplete information regarding the palaeogeographic setting (which typically becomes more acute with increasing age of the system), b) incomplete information regarding the evolution of individual structures (which typically becomes more acute with increasing deformation of the system). Within the Late Pleistocene Lisan Formation, the palaeogeographic setting is well constrained. In addition, the layer-cake stratigraphy, coupled with multiple slump events of varying intensity, allow the preservation of a whole range of structural features that are “frozen” at various stages of evolution and which permit distinct progressive deformation sequences to be established.

During initiation of slumping, upright “billows” and folds form at right angles to bedding and reflect layer-parallel shortening within the horizon coupled with density-driven perturbations. These folds are triggered by the initial seismic event and may be associated with Rayleigh–Taylor instabilities. Rayleigh–Taylor instability is generated by inverse density gradients (i.e. dense layers overlying less denser layers), with the lighter layer floating upwards when the system is shaken resulting in upright fold-like intrusions (e.g. Wetzler et al., 2010). The upright “billow” style of folding is restricted to thicker mud-rich horizons that are typically considered to have been rapidly deposited during winter storms. They may therefore trap significant volumes of water within them that would encourage density-driven instability and folding during seismic events.

Dasgupta (2008) notes that as the amplitude of folds increases, the apical angle reduces to a critical value of 120° at which point the Kelvin–Helmholtz (K–H) instability sets in with tongues of clay-rich sediment squeezing into sand. The K–H instability (in contrast

to the Rayleigh–Taylor instability noted above) is triggered by shear between layers, where the stratification is stable (less dense layers are at the top) and typically generates asymmetric folds via differences in velocity (similar to ocean waves generated by wind). Wetzler et al. (2010) suggested that the K–H instability is a plausible mechanism to explain some of the folding and brecciation within the Lisan Formation because it requires only a small perturbation in the interface between sheared layers, which then grows and evolves through folding stages up to a turbulent breccia. Although Wetzler et al. (2010) did not analyse fold vergence or the transport direction of the material, our work shows that the sense of slump transport is dictated by the palaeoslope. It should be noted that early upright folds associated with layer-parallel shortening have also been generated in sandbox models (Fig. 8) and in recent analogue experiments by Noble and Dixon (2011).

In the present case study folds, which are created during initiation of slumping noted above (e.g. Fig. 13a), are then carried on thrusts formed during the subsequent translation of the slump (Fig. 17b). This study demonstrates that thrusts typically get younger in the direction of slumping (i.e. a basin-ward propagating system of piggyback thrusts) as: a) Structurally higher thrusts are progressively back steepened as younger thrusts form beneath them (e.g. Fig. 17b); b) Synclines in the footwall of thrusts are also progressively “squeezed” and pinched closed as this back-steepening continues; c) Secondary thrusts may branch off each individual thrust as it forms, and are themselves progressively back steepened along with the “host” thrust sheets (e.g. Fig. 17b). Thus, the upright “billow” folds are back-rotated (with the associated thrust plane that they root downwards onto) and therefore formed before imbrication, but during the same progressive deformation event associated with slump translation (Figs. 8, 13b and 17b). After upright folds are rotated on back-steepened thrust planes, new approximately vertical folds start to form suggesting that gravity-driven instability together with horizontal compression continue to operate and are the driving force. Foreland (or downslope) propagation of fold and thrust systems that cut through early upright folds has also been generated in analogue models (Noble and Dixon, 2011).

Upright folds growing off thrust imbricates may reflect late-stage horizontal compression associated with cessation of slump movement (Fig. 17c). The crests of these folds may develop outward verging geometries to form “mushroom” headed folds. Vergence directed away from the crest is considered to reflect a phase of secondary slumping or relaxation within the slump and is marked by thinning of horizons over culminations and concomitant thickening in troughs (Fig. 17c). The mushroom headed geometry of these folds may be further amplified by vertical compression associated with loading from overlying sediments during slump compaction (Fig. 17c). Locally, this late-stage compaction is marked by sub-horizontal contractional crenulations within upright beds.

In summary, initial upright folds associated with layer shortening and density instabilities are carried on thrust imbricates as they translate downslope. The progressive steepening and systematic back rotation of imbricates indicates that they typically formed sequentially and consecutively, rather than as out of sequence or concurrent systems of thrusts in which such

downslope flow direction. Both the lower folded sequence and the overlying thrust system are subsequently cut by a sedimentary injection (centre of photograph) sourced from an immediately underlying slumped unit. b) Photograph showing slump-related imbricates which display progressive back-steepening towards the left (SW) at Peratzim. Upright folds are positioned above, and appear to root downwards onto each thrust. These folds are also rotated and therefore formed before imbrication, but during the same progressive deformation event. After upright folds are rotated on back-steepened thrust planes, new approximately vertical “billow” folds form c) Summary photograph from Peratzim illustrating early folds (by coin) formed during initiation of slumping that have been subsequently refolded by thrust-related recumbent folds (during slump translation). Upright folds then grow off the thrusts reflecting horizontal compression (during slump cessation) which themselves develop outward verging geometries to form “mushroom” headed folds (during slump relaxation). These mushroom headed folds are amplified by sub-horizontal contractional crenulations of upright beds (during slump compaction). All features are cut by steep sedimentary injections. d) Photograph showing the details of a detachment fold associated with downslope slumping towards the NE at Peratzim. The cores of the detachment folds are filled by mud-rich sediment, with more competent (lighter) overlying layers displaying local thrusts.

systematic back-steepening of each imbricate compared to its immediate neighbour is unlikely (Fig. 17b). Subsequent cessation, relaxation and compaction of the slump sheet may then superimpose a distinct sequence of progressive structural features on each slumped unit.

7.3. Why are the tops of slumps apparently truncated?

Structures generated during slump translation and cessation are often seen to be truncated by overlying undeformed horizontal beds that cap the slump, with apparently truncated tops to folded packages reported by Woodcock (1976b); Farrell (1984); Farrell and Eaton (1988); Maltman (1994b,c); and Strachan (2008). Within the case study area, the top surfaces of slumps are locally marked by apparently truncating surfaces in which the slumped material is thinned and removed, and directly overlain by a capping bed of marl or mud (Fig. 5c). This overlying bed locally thins over structural culminations in the underlying slump (Fig. 13e). Erosive truncation by a scouring turbidity current is considered unlikely in this instance as a waning turbidity flow should deposit coarse turbidity-related sediment (e.g. Kneller, 1995). However, as noted the overlying sediment is typical fine-grained Lisan marls and muds. Equally, truncation by thrusts is considered unlikely because: a) No evidence of faulting exists either along these contacts nor are any thrust imbricates observed branching off the contact. b) Such a model would necessitate the entire overlying sequence to be allochthonous and carried on this basal thrust. There is no deformation in the overlying sequence to support this. c) Sediment thickening and thinning associated with growth patterns that directly link to underlying culminations in the slump do not support such an allochthonous thrust model.

We therefore suggest that the top surfaces have been largely “levelled” by flow off culminations produced during the earlier slump event. This relaxation results in thinning of material off “highs” and thickening into troughs as is observed. It also corresponds to secondary slump folds verging away from the crests of earlier slumps (e.g. Fig. 13e). The thinning of capping beds over underlying culminations suggests that any readjustment by secondary slumping was incomplete and a weak bathymetry survived that controlled initial deposition of the overlying sequence.

7.4. Why are older slumped sequences reworked by younger events?

It has long been thought that some slump sheets may be “composite” and comprise more than one slump event (e.g. Woodcock, 1979), although recognising clear criteria for the separation of multiple slump events within single slump sheets is more problematic. The situation is further complicated as each seismic event may trigger a progressive deformation sequence (see Section 7.2.) where early structures are continually reworked during slump translation and cessation, and which ultimately produces a non-unique deformation history, i.e. each slump cycle may display a similar pattern and relative history of deformation as its neighbour. The problems faced are not unlike those experienced in high-grade metamorphic terranes where unravelling complex deformation (D) chronologies advanced significantly when it was realised that similar relative histories may be generated at slightly different times in the same thrust sheet or adjacent nappes and regions. The importance of such detailed “unravelling” of multiple events within slump sheets is highlighted by the concerns of palaeoseismologists who may miss seismic events due to multiple seismic triggers hidden within individual slumped units. The net effect of this

“miscounting” would be to over estimate the recurrence interval of earthquakes and hence to underestimate the seismicity of an area.

There is no intrinsic reason as to why seismically-triggered slumping should only affect the uppermost package of sediment deposited since the last earthquake (see Section 6). If seismicity is relatively frequent compared to (slow) deposition of sediments, then it may be more likely to affect underlying pre-existing slumped sediment sequences as well (i.e. slumped packages may have been reactivated and/or have some folds amplified). However, in many cases slumped units are typically <1 m thick and detach on underlying horizons which remain largely undeformed. The presence of these underlying and undeformed horizontal beds demonstrates that deformation has not penetrated and reworked deeper pre-existing slumped horizons. The reason for this continual deformation of “new” sediment packages may reflect the fact that detachment surfaces will typically find it easier to propagate along weak horizons within the flat, but mechanically heterogeneous, layer-cake stratigraphy rather than cut across pre-existing folds and structures. In addition, older slumps will become progressively compacted and lithified.

Although Marco et al. (1996) realised that some seismite layers may be the product of more than one seismic event, their calculations assumed that each brecciated seismite layer represents a separate >5.5 magnitude event. Marco et al. (1996) calculated that the long term recurrence interval of such events is about 1.6 kyr with ~30 layers recorded in the 50 kya interval of the Lisan Formation. Based on detailed observations of deformation within slumped horizons, thickness of brecciated horizons, coupled with evidence of some structures being traceable from one horizon to another, we currently estimate that up to 10% of slumped units may in fact be the product of multiple (i.e. double) seismic events. Clearly the recurrence interval of >5.5 m events may be less than originally estimated, although exact calculations require further detailed structural analysis on individual logged sections through the Lisan Formation.

7.5. Why are strike-slip shear zones on the margins of slumps not observed ?

It is interesting to note that the classical flow perturbation models of Coward and Potts (1983) and Farrell (1984) suggest that the lateral margins of slumps should be marked by zones of differential shear associated with strike-slip faults (Fig. 1). Within this case study however, such transport-parallel zones of differential movement have not been identified, despite high quality exposure that would intersect these downslope trending shears. The lack of observed strike-slip zones may reflect a number of factors described below.

- Reworked zones of differential shear have been overprinted and destroyed by contraction and extension associated with neighbouring slump sheets. However, we have not identified any structures associated with such reworking of slump sheets and therefore feel that this is unlikely in this case.
- Diffuse zones of differential shear where displacement is pervasively distributed across a broad zone of sediment making the observation of individual strike-slip structures difficult. We feel that this is unlikely as both contractional and extensional related structures generate discrete folds and thrusts.
- Discrete zones of differential shear in which transpressional/transensional domains towards the toe and head are partitioned into contractional/extensional structures containing extremely localised strike-slip domains. We feel that the lack of

direct observation of such structures makes a partitioned transpression/transension model unlikely.

- d) Widely spaced zones of differential shear reflecting the shape of the primary slump cell. Slumps which extend for long distances along-strike compared to their downslope extent will have a much smaller proportion of their overall margin dominated by differential shear. [Alsop and Holdsworth \(2007\)](#) have classified such flow cells according to their length/width aspect ratio (measured parallel to flow) as <1 . They are more likely to occur in laterally unconfined slump sheets (which encourages the along-strike propagation of slumps) and those associated with homogeneous layer-cake stratigraphy which does not encourage the development of individual flow lobes separated by zones of differential shear. We feel that this is the most likely explanation for the lack of differential shear zones in the slumps examined at Peratzim.

7.6. Why are relatively thin slump sheets generated over large areas?

Within the present case study, the overall 3-D geometry of slump sheets is difficult to fully ascertain due to the limitations of continuous across-strike exposure in wadi-dominated settings. At Peratzim, individual slump sheets are relatively thin (typically $<1\text{--}2$ m thick) but may be confidently correlated along strike over distances of at least 250 m. The thickness to along-strike width ratios of slumped sheets is therefore in the order of $1:\gt 100$. These thin, but extensive along-strike slump sheets are marked by a lack of folds generated oblique or parallel to the flow direction, suggesting that layer-normal shear associated with differential downslope movement does not typically occur (see [Alsop and Holdsworth, 2007](#); [Debacker et al., 2009](#)). The overall control reflects the thin layer-cake stratigraphy which contains little lateral variation to encourage partitioning and differential shear in the sheet. The thin layers (in some cases on a mm-scale) encourage numerous small cylindrical folds and structures which do not have large amplitudes and which do not cause significant thickening of the slumped sheet. The layer-cake stratigraphy coupled with the cylindrical nature of these folds will also encourage uniform fold wavelength – height ratios across a range of scales as recently recognised by [Wetzler et al. \(2010\)](#).

8. Conclusions

This project has involved the careful measuring and recording of the 3-D geometry of a range of truly exceptional sedimentary slump structures developed within the Late Pleistocene Lisan Formation along the western Dead Sea margin. Our observations enable us to draw the following conclusions.

8.1. Distinguishing overprinting scenarios during progressive evolution of slumps

It is possible to generate a range of 4 broad overprinting scenarios within a single slump event depending on a) if the observations are made towards the toe or head of an individual slump, and b) if cessation of the slump initiates first at the head (leading to superimposed extensional strain) or toe (leading to superimposed contractional strain). We have also recognised that the progressive evolution of slump systems may be categorised into initiation, translation, cessation, relaxation and compaction phases. Secondary slumping associated with flow directly off structural culminations created during the translation of slump sheets may create folds and thrusts which locally verge back up the

palaeoslope. The examination of these structures in isolation would provide an incorrect palaeoslope interpretation.

8.2. Distinguishing thrust and fold sequences

Thrust packages typically define piggyback sequences with back-steepening of imbricate faults. Pronounced back steepening may facilitate collapse of folds back up the regional palaeoslope. The development of piggyback thrust sequences during the translation of the slump sheet is different to previous models which suggest that thrusts were generated much later during cessation of movement (e.g. [Farrell, 1984](#); [Strachan, 2008](#)), and involve an overstep sequence as contraction propagates back upslope through the slump sheet.

8.3. Distinguishing reworking within slumps by multiple events

A number of separate movement horizons are observed indicating several discrete slump “events”. Slumped units are generally separated by undeformed horizontal strata. This deformation is considered to be triggered by earthquakes associated with seismicity along the Dead Sea transform. Extensional faults may be reactivated and reworked during subsequent (seismic) events related to continued failure and slumping. Careful structural evaluation of slumped horizons may also permit structural linkages to be recognised across apparently separate and distinct slumped units. The recognition that up to 10% of slumps may be reworked by younger seismically-triggered events suggests that in some cases the seismic recurrence interval may be shorter than previously estimated.

8.4. Distinguishing contractional structures that may be “hidden” on seismic

The recognition of detailed contractional fold and thrust structures, together with bedding-parallel detachments may be useful in explaining some of the contractional strain typically found to be “missing” when attempts are made to balance large-scale structures observed in gravity-driven mass transfer complexes (e.g. see [Butler and Paton, 2010](#)). Upright folding is found to be rotated along back-steepened thrusts indicating it pre-dates thrusting and represents a phase of early layer-parallel shortening. As the system effectively infills back to the horizontal and resets after each slump event, the relatively small scale contractional structures may be difficult to identify on seismic sections as they maintain broadly horizontal boundaries. It should also be noted that a) there is no necessity for adjacent slump complexes to balance as they form non-linked systems, b) the development of conjugate faults sub-parallel to flow indicates non-plane strain deformation and out of section movement. These observations may collectively help account for some of the “hidden” contraction typically encountered during seismic interpretation of basin-scale sections.

Acknowledgements

We thank Mr. John Levy, together with the Carnegie Trust and the Royal Society of Edinburgh for travel grants to IA, and the Israel Science Foundation for grant 1539/08 to SM. We thank Xavier Fort for discussion and permission to use one of his experiments, together with the referees and editor, Nigel Woodcock and Bob Holdsworth, for careful and constructive reviews. SM would like to acknowledge the Department of Earth Sciences at Durham University for hosting him and facilitating the completion of this paper.

References

- Aftabi, P., Roustai, M., Alsop, G.I., Talbot, C.J., 2010. InSAR mapping and modelling of an active Iranian salt extrusion. *Journal of the Geological Society, London* 167, 155–170.
- Agnon, A., Migowski, C., Marco, S., 2006. Intraclast breccia layers in laminated sequences: recorders of paleo-earthquakes. In: Enzel, Y., Agnon, A., Stein, M. (Eds.), *New Frontiers in Dead Sea Paleoenvironmental Research*. Geological Society of America Special Publication, pp. 195–214.
- Alsop, G.I., Carreras, J., 2007. Structural evolution of sheath folds: a case study from Cap de Creus. *Journal of Structural Geology* 29, 1915–1930.
- Alsop, G.I., Holdsworth, R.E., 2002. The geometry and kinematics of flow perturbation folds. *Tectonophysics* 350, 99–125.
- Alsop, G.I., Holdsworth, R.E., 2004a. The geometry and topology of natural sheath folds: a new tool for structural analysis. *Journal of Structural Geology* 26, 1561–1589.
- Alsop, G.I., Holdsworth, R.E., 2004b. Shear zone folds: records of flow perturbation or structural inheritance? In: Alsop, G.I., Holdsworth, R.E., McCaffrey, K.J.W., Hand, M. (Eds.), *Flow Processes in Faults and Shear Zones*. Geological Society, London, Special Publications, vol. 224, pp. 177–199.
- Alsop, G.I., Holdsworth, R.E., 2006. Sheath folds as discriminators of bulk strain type. *Journal of Structural Geology* 28, 1588–1606.
- Alsop, G.I., Holdsworth, R.E., 2007. Flow perturbation folding in shear zones. In: Ries, A.C., Butler, R.W.H., Graham, R.D. (Eds.), *Deformation of the Continental Crust: The Legacy of Mike Coward*. Geological Society, London, Special Publications, vol. 272, pp. 77–103.
- Alsop, G.I., Holdsworth, R.E., McCaffrey, K.J.W., 2007. Scale invariant sheath folds in slumps, sediments and shear zones. *Journal of Structural Geology* 29, 1585–1604.
- Begin, Z.B., Ehrlich, A., Nathan, Y., 1974. Lake Lisan, the Pleistocene precursor of the Dead sea. *Geological Survey of Israel Bulletin* 63, 30.
- Bradley, D., Hanson, L., 1998. Paleoslope analysis of slump folds in the Devonian flysch of Main. *The Journal of Geology* 106, 305–318.
- Bull, S., Cartwright, J., Huuse, M., 2009. A review of kinematic indicators from mass-transport complexes using 3D seismic data. *Marine and Petroleum Geology* 26, 1132–1151.
- Butler, R.W.H., Paton, D.A., 2010. Evaluating lateral compaction in deepwater fold and thrust belts: how much are we missing from Natures sandbox? *GSA Today* 20, 4–10.
- Collinson, J., 1994. Sedimentary deformational structures. In: Maltman, A.J. (Ed.), *The Geological Deformation of Sediments*. Chapman & Hall, London, pp. 95–125.
- Coward, M.P., Potts, G.J., 1983. Complex strain patterns developed at the frontal and lateral tips to shear zones and thrust zones. *Journal of Structural Geology* 5, 383–399.
- Dasgupta, P., 2008. Experimental decipherment of the soft-sediment deformation observed in the upper part of the Talchir Formation (Lower Permian), Jharia Basin, India. *Sedimentary Geology* 205, 100–110.
- Davis, G.H., Reynolds, S.J., 1996. *Structural Geology of Rocks and Regions*, second ed. John Wiley and Sons, New York, 776 pp.
- Debacker, T.N., Sintubin, M., Verniers, J., 2001. Large-scale slumping deduced from structural and sedimentary features in the Lower Palaeozoic Anglo-Brabant fold belt, Belgium. In: *Journal of the Geological Society of London*, vol. 158 341–352.
- Debacker, T.N., Dumon, M., Matthys, A., 2009. Interpreting fold and fault geometries from within the lateral to oblique parts of slumps: a case study from the Anglo-Brabant Deformation Belt (Belgium). *Journal of Structural Geology* 31, 1525–1539.
- Druguet, E., Alsop, G.I., Carreras, J., 2009. Coeval brittle and ductile structures associated with extreme deformation partitioning in a multilayer sequence. *Journal of Structural Geology* 31, 498–511.
- Elliot, C.G., Williams, P.F., 1988. Sediment slump structures: a review of diagnostic criteria and application to an example from Newfoundland. *Journal of Structural Geology* 10, 171–182.
- El-Isa, Z.H., Mustafa, H., 1986. Earthquake deformations in the Lisan deposits and seismotectonic implications. In: *Geophysical Journal of the Royal Astronomical Society*, vol. 86 413–424.
- Farrell, S.G., 1984. A dislocation model applied to slump structures, Ainsa Basin, South Central Pyrenees. *Journal of Structural Geology* 6, 727–736.
- Farrell, S.G., Eaton, S., 1987. Slump strain in the Tertiary of Cyprus and the Spanish Pyrenees. Definition of palaeoslopes and models of soft sediment deformation. In: Jones, M.F., Preston, R.M.F. (Eds.), *Deformation of Sediments and Sedimentary Rocks*. Special Publication of the Geological Society of London, vol. 29, pp. 181–196.
- Farrell, S.G., Eaton, S., 1988. Foliations developed during slump deformation of Miocene marine sediments, Cyprus. *Journal of Structural Geology* 10, 567–576.
- Garfunkel, Z., 1981. Internal structure of the Dead Sea leaky transform (rift) in relation to plate kinematics. *Tectonophysics* 80, 81–108.
- Gilbert, L., Sanz de Galdeano, C., Alfaro, P., Scott, G., Lopez Garrido, A.C., 2005. Seismic-induced slump in early Pleistocene deltaic deposits of the Baza basin (SE Spain). *Sedimentary Geology* 179, 279–294.
- Hansen, E., 1971. *Strain Facies*. Springer-Verlag, Berlin, 207 pp.
- Haase-Schramm, A., Goldstein, S.L., Stein, M., 2004. U-Th dating of Lake Lisan aragonite (late Pleistocene Dead Sea) and implications for glacial East Mediterranean climate change. *Geochimica et Cosmochimica Acta* 68, 985–1005.
- Heifetz, E., Agnon, A., Marco, S., 2005. Soft sediment deformation by Kelvin Helmholtz instability: a case from Dead Sea earthquakes. *Earth and Planetary Science Letters* 236, 497–504.
- Holdsworth, R.E., 1988. The stereographic analysis of facing. *Journal of Structural Geology* 10, 219–223.
- Holdsworth, R.E., 1990. Progressive deformation structures associated with ductile thrusts in the Moine Nappe, Sutherland, N. Scotland. *Journal of Structural Geology* 12, 443–452.
- Ken-Tor, R., Agnon, A., Enzel, Y., Marco, S., Negendank, J.F.W., Stein, M., 2001. High-resolution geological record of historic earthquakes in the Dead Sea basin. *Journal of Geophysical Research* 106, 2221–2234.
- Kneller, B., 1995. Beyond the turbidite paradigm: physical models for deposition of turbidites and their implications for reservoir prediction. In: Hartley, A.J., Prosser, D.J. (Eds.), *Characterization of Deep Marine Clastic Systems*. Geological Society, London, Special Publications, vol. 94, pp. 31–49.
- Lajoie, J., 1972. Slump fold axis orientations: an indication of Palaeoslope? *Journal of Sedimentary Petrology* 42, 584–586.
- Lesemann, J.-E., Alsop, G.I., Piotrowski, J.A., 2010. Incremental subglacial meltwater sediment deposition and deformation associated with repeated ice-bed decoupling: a case study from the Island of Funen, Denmark. *Quaternary Science Reviews* 29, 3212–3229.
- Levi, T., Weinberger, R., Eyal, Y., 2011. A coupled fluid-fracture approach to propagation of clastic dikes during earthquakes. *Tectonophysics* 498, 35–44.
- Lewis, K.B., 1971. Slumping on a continental slope inclined at 1–4°. *Sedimentology* 16, 97–110.
- Maltman, A., 1984. On the term soft-sediment deformation. *Journal of Structural Geology* 6, 589–592.
- Maltman, A., 1994a. *The Geological Deformation of Sediments*. Chapman & Hall, London, 362 pp.
- Maltman, A., 1994b. Introduction and overview. In: Maltman, A. (Ed.), *The Geological Deformation of Sediments*. Chapman & Hall, London, pp. 1–35.
- Maltman, A., 1994c. Deformation structures preserved in rocks. In: Maltman, A. (Ed.), *The Geological Deformation of Sediments*. Chapman & Hall, London, pp. 261–307.
- Marrett, R., Peacock, D.C.P., 1999. Strain and stress. *Journal of Structural Geology* 21, 1057–1063.
- Marco, S., Agnon, A., 1995. Prehistoric earthquake deformations near Masada, Dead Sea graben. *Geology* 23, 695–698.
- Marco, S., Stein, M., Agnon, A., Ron, H., 1996. Long term earthquake clustering: a 50,000 year palaeoseismic record in the Dead Sea graben. *Journal of Geophysical Research* 101, 6179–6192.
- Marco, S., Weinberger, R., Agnon, A., 2002. Radial clastic dykes formed by a salt diapir in the Dead Sea Rift, Israel. *Terra Nova* 14, 288–294.
- Martinsen, O.J., 1989. Styles of soft-sediment deformation on a Namurian delta slope, western Irish Namurian basin, Ireland. In: Whateley, M.K.G., Pickering, K.T. (Eds.), *Deltas: Sites and Traps for Fossil Fuels*. Geol. Soc. London Spec. Publ., vol. 41, pp. 167–177 (Geological Society London, London).
- Martinsen, O.J., 1994. Mass Movements. In: Maltman, A. (Ed.), *The Geological Deformation of Sediments*. Chapman & Hall, London, pp. 127–165.
- Martinsen, O.J., Bakken, B., 1990. Extensional and compressional zones in slumps and slides in the Namurian of County Claire, Eire. In: *Journal of the Geological Society of London*, vol. 147 153–164.
- Migowski, C., Agnon, A., Bookman, R., Negendank, J.F.W., Stein, M., 2004. Recurrence pattern of Holocene earthquakes along the Dead Sea transform revealed by varve-counting and radiocarbon dating of lacustrine sediments. *Earth and Planetary Science Letters* 222, 301–314.
- Noble, T.E., Dixon, J.M., 2011. Structural evolution of fold-thrust structures in analog models deformed in a large geotechnical centrifuge. *Journal of Structural Geology* 33, 62–77.
- Porat, N., Levi, T., Weinberger, R., 2007. Possible resetting of quartz OSL signals during earthquakes – evidence from late Pleistocene injection dikes, Dead Sea basin, Israel. *Quaternary Geochronology* 2, 272–277.
- Ridley, J., 1986. Parallel stretching lineations and fold axes oblique to displacement direction – a model and observations. *Journal of Structural Geology* 8, 647–654.
- Rowen, M.G., Peel, F.J., Vendeville, B.C., 2004. Gravity-driven fold-belts on passive margins. In: McClay, K.R. (Ed.), *Thrust Tectonics and Hydrocarbon Systems*. AAPG Memoir, 82, pp. 157–182.
- Smith, J.V., 2000. Flow pattern within a Permian submarine slump recorded by oblique folds and deformed fossils, Ulladulla, south-eastern Australia. *Sedimentology* 47, 357–366.
- Stewart, S.A., Clark, J.A., 1999. Impact of salt on the structure of the Central North Sea hydrocarbon fairways. In: Fleet, A.J., Boldy, S.A.R. (Eds.), *Petroleum Geology of Northwest Europe: Proceedings of the 5th Conference*. The Geological Society, London, pp. 179–200.
- Strachan, L.J., 2002. Slump-initiated and controlled syndepositional sandstone remobilization; an example from the Namurian of County Clare, Ireland. *Sedimentology* 49, 25–41.
- Strachan, L.J., 2008. Flow transformations in slumps: a case study from the Waitemata Basin, New Zealand. *Sedimentology* 55, 1311–1332.
- Strachan, L.J., Alsop, G.I., 2006. Slump folds as estimators of palaeoslope: a case study from the Fisherstreet Slump of County Clare, Ireland. *Basin Research* 18, 451–470.

- Van der Pluijm, B.A., Marshak, S., 2004. *Earth Structure: An Introduction to Structural Geology and Tectonics*, second ed. W.W. Norton & Company Ltd, New York, London, 656 pp.
- Waldron, J.W.F., Gagnon, J-F., 2011. Recognizing soft-sediment structures in deformed rocks of orogens. *Journal of Structural Geology* 33, 271–279.
- Wetzler, N., Marco, S., Heifetz, E., 2010. Quantitative analysis of seismogenic shear-induced turbulence in lake sediments. *Geology* 38, 303–306.
- Woodcock, N.H., 1976a. Ludlow series slumps and turbidites and the form of the Montgomery trough, Powys, Wales. *Proceedings of the Geologists Association* 87, 169–182.
- Woodcock, N.H., 1976b. Structural style in slump sheets: Ludlow series, Powys, Wales. In: *Journal of the Geological Society, London*, vol. 132 399–415.
- Woodcock, N.H., 1979. The use of slump structures as palaeoslope orientation estimators. *Sedimentology* 26, 83–99.